

A new method to calculate the n -Particle Irreducible Effective Action

M.E. Carrington* and Yun Guo†
Department of Physics, Brandon University,
Brandon, Manitoba, R7A 6A9 Canada
and
Winnipeg Institute for Theoretical Physics,
Winnipeg, Manitoba, Canada

In this paper, we present a new method to calculate the n -Loop n -particle irreducible effective action. The key is an organizational trick that involves the introduction of a set of fictitious bare vertices that are set to zero at the end of the calculation. Using these fictitious vertices, we prove that the Schwinger-Dyson equations are the same as the equations of motion obtained from the n -particle irreducible effective action, up to the level at which they respect the symmetries of the original theory. This result allows us to obtain the effective action directly from the Schwinger-Dyson equations, which are comparatively easy to calculate. As a check of our method, we reproduce the known results for the n -Loop n -particle irreducible effective action with $n = 4$ and $n = 5$. We also use the technique to calculate the 6-Loop 6-particle irreducible effective action.

I. INTRODUCTION

An n -Loop n -particle irreducible (n PI) effective theory is defined in terms of n functional arguments which correspond to a set of n -point functions that are determined self-consistently through a variational procedure. The idea was introduced in Refs. [1, 2] and first discussed in the context of relativistic field theories in Ref. [3]. The variational procedure resums certain classes of diagrams, and represents a reorganization of perturbation theory. n PI approximation schemes are especially interesting because they can be used to study far-from-equilibrium systems [4–9], which is of interest in the context of heavy ion collisions and cosmology. The potential importance of n PI theories is demonstrated by the fact that they can be used to formulate the calculation of transport coefficients [10–12]. To date however, numerical calculations have only been done for 2PI theories where it has been shown that the convergence of perturbative approximations is improved (see [13–15] and references therein). In addition, there are unresolved issues for gauge theories [16, 17]. The renormalizability of a theory is related to the existence of symmetry constraints on the n -point functions. For n PI effective theories, symmetries and renormalizability are connected to the fact that proper n -point functions can be defined in more than one way. All definitions are completely equivalent for the exact theory, but they are not the same at finite approximation order. These issues are well understood for scalar theories and QED at the 2PI level. For scalar theories, one can define a 2-point function that satisfies Goldstone’s theorem in the broken phase [18, 19]. For QED, one can define n -point functions that obey Ward identities [20–22]. These symmetry constraints allow one to construct a renormalized theory that preserves the symmetries of the original theory [19, 23–26]. For non-Abelian theories, the situation is more involved. It has been shown that at any order in the approximation scheme, the gauge dependence of the effective action always appears at higher approximation order [27, 28]. However, the gauge symmetries of the n -point functions are more complicated than for Abelian theories, and renormalizability remains an open question.

In this paper, we introduce a new method to calculate the n PI effective action. While it is true in principle that the effective action can always be obtained from a series of Legendre transforms, this method is extremely complicated for $n > 3$, and probably prohibitively tedious beyond $n = 5$.

* carrington@brandonu.ca

† guoyun@brandonu.ca

The 3-Loop 4PI effective action was calculated in Refs. [1, 2, 29, 30], the 4-Loop 4PI effective action in Ref. [12], and the 5-Loop 5PI effective action in Ref. [31]. The key to our method is the introduction of a set of fictitious bare vertices: to obtain the n -Loop n PI effective action we include in the Lagrangian the vertices V_j^{oo} for $j = 3, 4, 5, 6, \dots, n$. The inclusion of the nonrenormalizable interactions ($j \geq 5$) is an organizational trick, and these vertices will be set to zero at the end of the calculation. Using these fictitious vertices, we can show that the equations of motion (eom's) and Schwinger-Dyson (sd) equations are equivalent to the order at which the truncated theory respects the symmetries of the original theory. This result allows us to construct the n -Loop n PI effective action directly from the sd equations.

This paper is organized as follows. In Sec. II, we define our notation. In Sec. III, we discuss the basic structure of the n PI effective action. In Sec. IV, we prove that the eom's and sd equations are equivalent to the truncation order. Our new method to calculate the effective action is explained in detail in Sec. V. In Secs. VI and VII, we show how to reproduce, with comparatively little effort, the known results for the n -Loop n PI effective action with $n = 4$ and $n = 5$. This provides a check of the procedure. In Sec. VIII, we use the technique to calculate the 6-Loop 6PI effective action which is, realistically speaking, impossibly tedious to obtain using Legendre transforms.

We make one further comment. Our method is based on the fact that using fictitious vertices in intermediate steps of the calculation, the sd equations can be rewritten so that they have the same structure as the eom's. It is important to realize that this result is important *only* because it allow us to obtain the effective action without taking a series of Legendre transforms. It is *not* true that the nonperturbative solutions of a truncated set of sd equations are the same as the solutions of the eom's obtained from the n PI effective action.

II. NOTATION

Throughout this paper we use L to indicate the loop order in the skeleton expansion. We also use “ n -Loop” to mean terms in the skeleton expansion with $L \leq n$ loops, and “ n -loop” to mean terms in the skeleton expansion with $L = n$ loops. We consider only scalar theories. The generalization of the method to other theories is straightforward.

In most equations in this paper, we suppress the arguments that denote the space-time dependence of functions. As an example of this notation, the quadratic term in the action is written [see Eq. (4)]:

$$\frac{1}{2} \int d^4x d^4y \varphi(x) [i(D^{oo})^{-1}(x-y)] \varphi(y) \rightarrow \frac{i}{2} (D^{oo})^{-1} \varphi^2. \quad (1)$$

We define several different kinds of vertex functions and use the letter V for all of them, with a single subscript denoting the number of legs:

$$\begin{aligned} V_j^{oo} & \text{ bare vertex - equation (4),} \\ V_j^0 & \text{ effective bare vertex - equation (6),} \\ V_j^c & \text{ connected vertex - equation (8),} \\ V_j & \text{ proper vertex - equation (9),} \\ \tilde{V}_j & \text{ tilde vertex - equation (10).} \end{aligned} \quad (2)$$

Unless stated otherwise, the indices $\{j, k, l, \dots\}$, which indicate the number of legs on a bare, effective bare, connected, proper, or tilde vertex, run from 3 to n . In diagrams, bare vertices and proper

vertices are denoted by open circles and solid dots, respectively¹. Many of the equations we will write in this paper are easier to understand as diagrams. In some cases, we will give only the diagrammatic form of an equation.

To illustrate a limitation of our notation, we write the equation that relates the 4-point connected vertex to proper vertices without suppressing space-time arguments. We use a single index to denote a space-time variable, and the summation convention to mean integration. The standard result is

$$V_{ijkl}^c = D_{it_1} D_{jt_2} D_{kt_3} D_{lt_4} V_{t_1 t_2 t_3 t_4} + D_{it_1} D_{jt_2} D_{kt_3} D_{lt_4} D_{t_5 t_6} V_{t_1 t_6 t_3} V_{t_2 t_5 t_4} \\ + D_{it_1} D_{jt_2} D_{kt_3} D_{lt_4} D_{t_6 t_5} V_{t_1 t_2 t_6} V_{t_3 t_5 t_4} + D_{it_1} D_{jt_2} D_{kt_3} D_{lt_4} D_{t_6 t_5} V_{t_1 t_5 t_4} V_{t_6 t_2 t_3} . \quad (3)$$

Using our notation in which indices are suppressed, the distinction between the s , t , and u channels is lost and the second, third, and fourth terms on the right side become $(3)D^5V_3^2$. We indicate that all three channels are included in one term by writing the factor (3) in brackets. In all calculations, contributions to a given vertex that correspond to different permutations of external legs must be treated correctly. The abbreviated notation only allows us to present results in a simpler form.

We introduce some terminology for different types of graphs that could appear in the effective action.

Basketballs: Graphs with two V_j vertices which are connected by j propagators. A generic example is shown in part (a) of Fig. 1.

Tadpoles: Graphs that would produce disconnected contributions to the equation of motion of one of the vertices in the graph (which we call the “tadpole vertex”). Some examples are shown in part (b) of Fig. 1. Tadpole graphs with only 1 vertex [for example, part (b_1) in Fig. 1] are type (1), and all other tadpole graphs [for example, part (b_2) in Fig. 1] are type (2).

Flowers: Graphs that would produce nonproper (1PR) contributions to the equation of motion of one of the vertices in the graph (which we call the “flower vertex”). Some examples are shown in part (c) of Fig. 1.

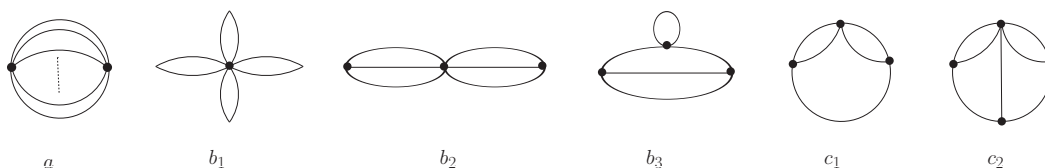


FIG. 1. Some of graphs that could appear in the effective action. In graph (b_1), the 8-point vertex is the tadpole vertex. In graph (b_2), the 6-point vertex is the tadpole vertex. In graph (c_1), the 4-point vertex is the flower vertex. In graph (c_2), the 5-point vertex is the flower vertex.

The effective action is calculated using a trick which involves introducing a set of fictitious bare vertices as an organizational tool. At the end of the calculation, the bare vertices are set to zero for $j \geq 5$. The classical action is

$$S_{cl}[\varphi] = \frac{1}{2}\varphi[i(D^{oo})^{-1}]\varphi - \sum_{j=3}^n \frac{i}{j!} V_j^{oo} \varphi^j . \quad (4)$$

¹ Figures in this paper are drawn using Jaxodraw [32].

It will be useful to define an effective bare propagator and effective j -point vertex as

$$(D^0(\phi))^{-1} = -i \frac{\delta^2 S_{cl}[\phi]}{\delta \phi^2}, \quad V_j^0(\phi) = i \frac{\delta^j S_{cl}[\phi]}{\delta \phi^j}. \quad (5)$$

From now on, we suppress the argument and write $D^0(\phi) \rightarrow D^0$ and $V_j^0(\phi) \rightarrow V_j^0$. The general relation between bare vertices V_j^{oo} and effective bare vertices V_j^0 is

$$V_l^0 = \sum_{j=l}^n \frac{1}{(j-l)!} V_j^{oo} \phi^{j-l}. \quad (6)$$

III. STRUCTURE OF THE EFFECTIVE ACTION

The n PI effective action is defined as the n th Legendre transformation of the connected generating functional which is constructed by coupling the field to n source terms:

$$Z[R_j] = \int d\varphi \text{Exp}[i(S_{cl}[\varphi] + \sum_{j=1}^n \frac{1}{j!} R_j \varphi^j)], \quad (7)$$

$$W[R_j] = -i \text{Ln} Z[R_j],$$

$$\Gamma[\phi, D, V_j^0, V_k] = W - \sum_{j=1}^n R_j \frac{\delta W}{\delta R_j}.$$

The last line in (7) gives the effective action as an implicit function of effective bare and proper vertices. We define connected green functions:

$$V_j^c = \langle \varphi^j \rangle_c = -(-i)^{j+1} \frac{\delta^j W}{\delta R_1^j}. \quad (8)$$

The equations that relate the connected and proper vertices are obtained from their definitions using the chain rule²

$$V_j = i \frac{\delta^j}{\delta \phi^j} \Gamma_{1\text{PI}} = i \frac{\delta^j}{\delta \phi^j} (W[R_1] - R_1 \phi). \quad (9)$$

We organize the calculation of the effective action using the method of subsequent Legendre transforms [29, 30]. This method involves starting from an expression for the 2PI effective action and exploiting the fact that the source terms R_j for $j \geq 3$ can be combined with the corresponding bare vertices by defining a set of modified interaction vertices which we call tilde vertices:

$$\tilde{V}_j := V_j^{oo} + i R_j. \quad (10)$$

Using these tilde vertices, we can rewrite the effective action in (7) as

$$\Gamma[\phi, D, V_j^0, V_k] =: \tilde{\Gamma}_{2\text{PI}} - \sum_{j=3} R_j \frac{\delta W}{\delta R_j}. \quad (11)$$

² Equations (8) and (9) are also valid for $j = 1, 2$. Equation (9) gives $V_2 = D^{-1}$ and thus $\Gamma[V_1, V_2, V_3 \dots V_n]$ really means $\Gamma[\phi, D^{-1}, V_3, V_4, \dots]$ and not $\Gamma[\phi, D, V_3, V_4, \dots]$. We ignore this point to avoid introducing unnecessary notation.

We will refer to $\tilde{\Gamma}_{2\text{PI}}$ as the tilded 2PI effective action. It is constructed from the complete set of n -Loop 2PI diagrams for a theory with bare vertices V_j^{oo} ($3 \leq j \leq n$) by replacing all bare vertices with tilde vertices³.

The 2PI effective action has the form

$$\Gamma_{2\text{PI}}[\phi, D, V_j^{oo}] = S_{cl}[\phi] + \frac{i}{2} \text{Tr} \text{Ln} D^{-1} + \frac{i}{2} \text{Tr} [(D^0)^{-1} D] - i\Phi[\phi, D, V_j^{oo}] + \text{const}, \quad (12)$$

where $\Phi[\phi, D, V_j^{oo}]$ contains all contributions to the effective action with two or more loops. It is convenient to divide the 0-loop and 1-loop contributions to $\tilde{\Gamma}_{2\text{PI}}$ into pieces that do and do not contain tilde vertices:

$$\begin{aligned} \tilde{\Gamma}_{2\text{PI}} &:= \Gamma_{2\text{PI}}[\phi, D, \tilde{V}_j] = \Gamma_0^{oo} + \tilde{\Gamma}_0 + \Gamma_1^{oo} + \tilde{\Gamma}_1 - i\tilde{\Phi}, \\ \Gamma_0^{oo} &= \frac{i}{2} (D^{oo})^{-1} \phi^2 \text{ contains 0-loop graphs with no tilde vertices,} \\ \tilde{\Gamma}_0 &= - \sum_{j=3}^n \frac{i}{j!} \tilde{V}_j \phi^j \text{ contains 0-loop graphs with tilde vertices,} \\ \Gamma_1^{oo} &= \frac{i}{2} \text{Tr} ((D^{oo})^{-1} D) + \frac{i}{2} \text{Tr} \text{Ln} D^{-1} \text{ contains 1-loop graphs with no tilde vertices,} \\ \tilde{\Gamma}_1 &= \frac{i}{2} \text{Tr} [(\tilde{D}^0)^{-1} - (D^{oo})^{-1}] D \text{ contains 1-loop graphs with tilde vertices,} \\ \tilde{\Phi} &= \Phi[\phi, D, \tilde{V}_j]. \end{aligned} \quad (13)$$

Using Eqs. (7), (8), (10), and (11), we have

$$\begin{aligned} \langle \phi^j \rangle &= j! \frac{\delta W}{\delta R_j} = j! \frac{\delta \tilde{\Gamma}_{2\text{PI}}}{\delta R_j} = ij! \frac{\delta \tilde{\Gamma}_{2\text{PI}}}{\delta \tilde{V}_j} \\ &=: V_j^c + \chi_j. \end{aligned} \quad (14)$$

The term χ_j contains all disconnected contributions to the expectation value, and is a function of connected vertices. A general expression for these terms is given in Appendix B. Substituting (10) and (14) into (11), we have

$$\Gamma[\phi, D, V_j^0, V_k] = \tilde{\Gamma}_{2\text{PI}} + \sum_{j=3}^n \frac{i}{j!} (V_j^c + \chi_j) (\tilde{V}_j - V_j^{oo}). \quad (15)$$

Using (13), Eq. (15) becomes

$$\begin{aligned} \Gamma[\phi, D, V_j^0, V_k] &= \Gamma_0^{oo} + \tilde{\Gamma}_0 + \Gamma_1^{oo} + \tilde{\Gamma}_1 \\ &\quad - i(\tilde{\Phi}_{\text{basketball}} + \tilde{\Phi}_{\text{tadpole}}^{(1)} + \tilde{\Phi}_{\text{tadpole}}^{(2)} + \tilde{\Phi}_{\text{flower}} + \tilde{\Phi}_{\text{rest}}) \\ &\quad + \sum_{j=3}^n \frac{i}{j!} \left(V_j^c + \chi_j^{(0)} + \chi_j^{(1)} + \chi_j^{(2)} + \chi_j^{(3)} \right) (\tilde{V}_j - V_j^{oo}), \end{aligned} \quad (16)$$

where we have separated contributions from the different types of graphs in $\tilde{\Phi}$ as discussed in Sec. II. The terms $\chi_j^{(i)}$ for $i=0,1,2$ refer to specific pieces of χ_j and $\chi_j^{(3)}$ includes all other contributions.

³ The only role of the fictitious vertices in a calculation using subsequent Legendre transforms is to introduce 2PI diagrams containing vertices V_j^{oo} for $5 \leq j \leq n$, which are then replaced by tilde vertices.

We give some examples that will be useful in the discussion below (see Appendix B):

$$\begin{aligned}
j=3: \quad & \chi_3^{(0)} = \phi^3, \quad \chi_3^{(1)} = (3)D\phi, \quad \chi_3^{(2)} = \chi_3^{(3)} = 0, \\
j=4: \quad & \chi_4^{(0)} = \phi^4, \quad \chi_4^{(1)} = (6)D\phi^2, \quad \chi_4^{(2)} = (3)D^2, \quad \chi_4^{(3)} = (4)V_3^c\phi, \\
j=5: \quad & \chi_5^{(0)} = \phi^5, \quad \chi_5^{(1)} = (10)D\phi^3, \quad \chi_5^{(2)} = (15)D^2\phi, \quad \chi_5^{(3)} = (5)V_4^c\phi + (10)V_3^c\phi^2 + (10)V_3^cD.
\end{aligned} \tag{17}$$

We define a functional that contains all terms in $\Gamma[\phi, D, V_j^0, V_k]$ that have bare vertices:

$$\Gamma^0[\phi, D, V_j^0, V_k] := \Gamma_0^{oo} + \Gamma_1^{oo} - \sum_{j=3}^n \frac{i}{j!} (V_j^c + \chi_j) V_j^{oo}. \tag{18}$$

The right side of (18) does not contain tilde vertices, and it is straightforward to convert connected vertices to proper ones, and bare vertices to effective bare vertices. The result has the form

$$\Gamma^0[\phi, D, V_j^0, V_k] =: S_{cl}[\phi] + \frac{i}{2} \text{Tr} \text{Ln} D^{-1} + \frac{i}{2} \text{Tr} [(D^0)^{-1} D] - i\Phi^0[V_j^0, V_k], \tag{19}$$

where $\Phi^0[V_j^0, V_k]$ contains all diagrams with more than one loop. The procedure is discussed in detail in Appendix C.

Using (B9) and the definitions in Eq. (13), it is straightforward to show

$$\begin{aligned}
\tilde{\Gamma}_0 + \sum_{j=3}^n \frac{i}{j!} \chi_j^{(0)} \tilde{V}_j &= 0, \\
\tilde{\Gamma}_1 + \sum_{j=3}^n \frac{i}{j!} \chi_j^{(1)} \tilde{V}_j &= 0, \\
-i\tilde{\Phi}_{\text{tadpole}}^{(1)} + \sum_{j=3}^n \frac{i}{j!} \chi_j^{(2)} \tilde{V}_j &= 0.
\end{aligned} \tag{20}$$

Substituting (18) and (20) into (16), we have

$$\begin{aligned}
& \Gamma[\phi, D, V_j^0, V_k] \\
&= \Gamma^0[\phi, D, V_j^0, V_k] - i(\tilde{\Phi}_{\text{basketball}} + \tilde{\Phi}_{\text{tadpole}}^{(2)} + \tilde{\Phi}_{\text{flower}} + \tilde{\Phi}_{\text{rest}}) + \sum_{j=3}^n \frac{i}{j!} (V_j^c + \chi_j^{(3)}) \tilde{V}_j.
\end{aligned} \tag{21}$$

Equation (21) is a formal result for the effective action as an implicit function of proper vertices. The right side is a function of tilde vertices and connected vertices. Comparing (21) with (15), we have

$$\tilde{\Gamma}_{2\text{PI}} = -i(\tilde{\Phi}_{\text{basketball}} + \tilde{\Phi}_{\text{tadpole}}^{(2)} + \tilde{\Phi}_{\text{flower}} + \tilde{\Phi}_{\text{rest}}) + \sum_{j=3}^n \frac{i}{j!} (\chi_j^{(3)} - \chi_j) \tilde{V}_j + \dots \tag{22}$$

where the dots represent terms that do not depend on \tilde{V}_j . Substituting into (14), we obtain

$$V_j^c = j! \frac{\delta}{\delta \tilde{V}_j} (\tilde{\Phi}_{\text{basketball}} + \tilde{\Phi}_{\text{tadpole}}^{(2)} + \tilde{\Phi}_{\text{flower}} + \tilde{\Phi}_{\text{rest}}) - \chi_j^{(3)}. \tag{23}$$

A generic basketball graph is shown in Fig. (1a). The associated symmetry factor for a graph with two \tilde{V}_j vertices is $(1/2)(1/j!)$. The first term on the right side of (23) therefore gives $D^j \tilde{V}_j$. Equation (23) can be solved iteratively to obtain an expression of the form

$$\tilde{V}_j = D^{-j} V_j^c + f_j[D, V_k^c], \tag{24}$$

which is valid to any desired loop order.

We define the interacting part of the effective action through the equation

$$\Gamma[\phi, D, V_j^0, V_k] =: \Gamma^0[\phi, D, V_j^0, V_k] - i\Phi^{\text{int}}[V_j]. \quad (25)$$

Using (21), we obtain

$$\Phi^{\text{int}}[V_j] = (\tilde{\Phi}_{\text{basketball}} + \tilde{\Phi}_{\text{tadpole}}^{(2)} + \tilde{\Phi}_{\text{flower}} + \tilde{\Phi}_{\text{rest}}) - \sum_{j=3}^n \frac{1}{j!} (V_j^c + \chi_j^{(3)}) \tilde{V}_j \quad (26)$$

We comment that Eq. (26) formally expresses $\Phi^{\text{int}}[V_j]$ as a functional of tilde and connected vertices. The procedure to obtain a functional of proper vertices is explained below.

The first step is to use Eq. (24) to remove the tilde vertices. We see immediately that this substitution gives

$$\sum_{j=3}^n \frac{1}{j!} V_j^c \tilde{V}_j \rightarrow 2 \sum_{j=3}^n \left[\frac{1}{2} \frac{1}{j!} V_j^c D^{-j} V_j^c \right] + \dots = 2\Phi_{\text{basketball}}^c + \dots \quad (27)$$

which causes the sign flip in the basketball diagrams on the right side of (26). We argue below that when all tilde vertices are removed the result is

$$\Phi^{\text{int}}[V_j] = -\Phi_{\text{basketball}}^c + \Phi_{\text{flower}}^c + \Phi_{\text{rest}}^c. \quad (28)$$

The function $\Phi_{\text{basketball}}^c$ represents the same set of basketball diagrams as $\tilde{\Phi}_{\text{basketball}}$ with tilde vertices replaced by connected vertices ($\tilde{V}_j \rightarrow D^{-j} V_j^c$). The function Φ_{flower}^c contains only graphs with flower topology, but not the same set of flower graphs as $\tilde{\Phi}_{\text{flower}}$. Similarly, Φ_{rest}^c contains only graphs that are not basketball, tadpole, or flower topologies, but not the same set of graphs as $\tilde{\Phi}_{\text{rest}}$. Recall that the tadpole graphs are those that produce disconnected contributions to the eom that corresponds to the tadpole vertex. It is clear that if a term of the form Φ_{tadpole}^c survived in Eq. (28), there would be a disconnected contribution to the eom for any connected vertex V_j^c which is a tadpole vertex. Since disconnected terms do not appear in the perturbative expansion [from the definition of connected vertices in Eq. (8)], they also do not appear in the skeleton expansion.

The connected vertex can be written in terms of proper vertices V_j using Eqs. (8) and (9). We will argue below that when we replace connected vertices with the appropriate expressions containing proper vertices, the flower graphs cancel and we obtain

$$\Phi^{\text{int}}[V_j] = -\Phi_{\text{basketball}} + \Phi_{\text{rest}}. \quad (29)$$

The function $\Phi_{\text{basketball}}$ contains basketball graphs which are functions of proper vertices. Φ_{rest} contains only graphs that are not basketball, tadpole, or flower topologies, but they are not the same graphs as in Φ_{rest}^c or $\tilde{\Phi}_{\text{rest}}$.

Consider the form of the eom obtained by functionally differentiating the effective action with respect to the vertex V_j . The effective action is obtained from Eqs. (25) and (29). For purposes of illustration, we rewrite the result as

$$\begin{aligned} \Gamma[\phi, D, V_j^0, V_k] &= \Gamma^0[\phi, D, V_j^0, V_k] - i(-\Phi_{\text{basketball}} + \Phi_{\text{rest}}) \\ &= S_d[\phi] + \frac{i}{2} \text{Tr} \text{Ln} D^{-1} + \frac{i}{2} \text{Tr} [(D^0)^{-1} D] - i(\Phi_{\text{basketball}}^0 + \Phi_{\text{no basketball}}^0 - \Phi_{\text{basketball}} + \Phi_{\text{rest}}), \end{aligned}$$

where we have split $\Phi^0[V_j^0, V_k]$ into two parts: $\Phi_{\text{basketball}}^0$ and $\Phi_{\text{no basketball}}^0$. In Appendix D, we show that, in $\Phi^{\text{int}}[V_j]$, the vertex V_j appears in one basketball diagram, and other diagrams which are higher loop order. Similarly, in $\Phi^0[V_j^0, V_k]$ (see Appendix C) the vertex V_j appears in the basketball

diagram with one proper vertex and one effective bare vertex, and other diagrams which are higher loop order. Using these results, and the fact that Φ_{rest} does not contain flower diagrams, the eom for the vertex V_j for $j \geq 3$ has the form

$$\begin{aligned} \frac{\delta\Gamma[\phi, D, V_j^0, V_k]}{\delta V_j} &= 0, \\ \Rightarrow j!D^{-j} \frac{\delta\Phi_{\text{basketball}}}{\delta V_j} &= j!D^{-j} \frac{\delta\Phi_{\text{basketball}}^0}{\delta V_j} + j!D^{-j} \frac{\delta\Phi_{\text{no basketballs}}^0}{\delta V_j} + j!D^{-j} \frac{\delta\Phi_{\text{rest}}}{\delta V_j}, \\ \Rightarrow V_j &= V_j^0 + \text{fcn}'_j[V_l^0, V_k] + \text{fcn}_j[V_k], \end{aligned} \quad (30)$$

where both $\text{fcn}'_j[V_l^0, V_k]$ and $\text{fcn}_j[V_k]$ contain only 1PI loop diagrams. The terms in the second and third lines of Eq. (30) are written in the same order. For example, the term V_j on the left side of the last equation comes from functionally differentiating the basketball diagram in Φ^{int} . If the flower topologies did not cancel when the effective action is written as a function of proper vertices, there would be a 1PR contribution to the eom for any proper vertex V_j which is a flower vertex. Since 1PR terms do not appear in the perturbative expansion [from the definition of proper vertices in Eq. (9)], they also do not appear in the skeleton expansion⁴.

Note that, for $j \geq 3$, there is no contribution from functionally differentiating the 1-Loop terms in $\Gamma^0[\phi, D, V_j^0, V_k]$ with respect to V_j . However, for $j = 2$, the 1-Loop terms in $\Gamma^0[\phi, D, V_j^0, V_k]$ do contribute, and produce the terms in the eom that correspond to V_j and V_j^0 on the left and right sides of Eq. (30), respectively.

IV. PROOF OF EQUIVALENCE OF THE EOM AND SD EQUATIONS

From this point on, we consider $\phi = 0$ for simplicity, which means that the bare vertices V_j^{oo} are equivalent to the effective bare vertices V_j^0 , and the bare propagator D^{oo} is equivalent to the effective bare propagator D^0 .

In this section, we show that the eom's produced by the n -Loop n PI effective theory are equivalent to the sd equations, up to the order at which they are consistent with the underlying symmetries of the original theory⁵. We comment that although both the n PI eom's and the sd equations are sets of coupled nonlinear integral equations that contain nonperturbative physics, there are significant differences between them. For an n PI effective theory, the effective action is truncated, and the resulting eom's form a closed set. In contrast, the sd equations form an infinite hierarchy of coupled equations which must be truncated in order to do calculations. In addition, there are fundamental differences in the basic structure of the two sets of equations. In the sd equation, all graphs contain one bare vertex and are not symmetric with respect to permutations of external legs. The n PI eom's are symmetric and (for $n > 2$) some graphs contain no bare vertices.

The first step is to compare the perturbative expansions of the sd equations and the eom's. In order to do this, we must use the equations of motion in (30), and also the corresponding equation for the 2-point function which is obtained from $\delta\Gamma/\delta D = 0$. The complete set of equations can be written

$$V_j = V_j^0 + \text{fcn}'_j[V_l^0, V_k] + \text{fcn}_j[V_k], \quad \{j, k, l\} \geq 2. \quad (31)$$

⁴ Tadpole and flower topologies are allowed in the part of the effective action that contains bare vertices, as long as the tadpole vertices and flower vertices are bare. For example, the EIGHT diagram is a tadpole, but the 4-point vertex is bare, and thus there is no disconnected contribution to the eom for the 4-point vertex from differentiating the EIGHT graph. Similarly, the HAIR graph is a flower diagram, but again the 4-point vertex is bare, and there is no 1PR contribution to the eom for the 4-point vertex.

⁵ For the 2-point function, one can show without using fictitious vertices that the eom from the n -Loop n PI effective action (for any n) and sd equation have exactly the same form. We prove this surprising result in Appendix E.

The definitions of the functions $\text{fcn}'_j[V_l^0, V_k]$ and $\text{fcn}_j[V_k]$ are given in Eq. (30) for $j \geq 3$. For $j = 2$, we have

$$j = 2 : \quad \text{fcn}'_2[V_l^0, V_k] = -2 \frac{\delta \Phi^0[V_l^0, V_k]}{\delta D}, \quad \text{fcn}_2[V_k] = -2 \frac{\delta \Phi^{\text{int}}[V_k]}{\delta D}. \quad (32)$$

If we define both terms in the 1-loop effective action to be 1-loop basketballs, the terms V_j and V_j^0 in (31) come from the functional derivative acting on the $(j - 1)$ -loop basketball graph, for each value of j . The sign difference for the 2-point function and the missing factor D^{-2} occurs because of the fact that it is conventional to write the effective action as a function of the propagator D instead of the inverse propagator D^{-1} (see footnote 2). To illustrate the notation, we write out Eq. (31) for $j = 2$ and $j = 3$:

$$\begin{aligned} \frac{\delta \Gamma[V_k]}{\delta D} = 0 & \rightarrow D^{-1} = (D^0)^{-1} - 2 \frac{\delta \Phi^0[V_l^0, V_k]}{\delta D} - 2 \frac{\delta \Phi^{\text{int}}[V_k]}{\delta D} \\ & =: (D^0)^{-1} - \Pi[V_k], \\ \frac{\delta \Gamma[V_k]}{\delta V_3} = 0 & \rightarrow V_3 = V_3^0 + 3! D^{-3} \frac{\delta \Phi_{\text{no basketballs}}^0[V_l^0, V_k]}{\delta V_3} + 3! D^{-3} \frac{\delta \Phi_{\text{rest}}}{\delta V_3} \\ & = V_3^0 + \text{fcn}'_3[V_l^0, V_k] + \text{fcn}_3[V_k]. \end{aligned} \quad (33)$$

We can generate the perturbative expansion of any functional of proper vertices by repeatedly substituting (31). We can also repackage a perturbative set of diagrams as skeleton diagrams that contain proper vertices by repeatedly using the same equation in the form

$$V_j^0 = V_j - \text{fcn}'_j[V_l^0, V_k] - \text{fcn}_j[V_k], \quad \{j, k, l\} \geq 2. \quad (34)$$

In the rest of this section, we use $\{j, k, l\} \geq 2$.

item 1: If we convert a set of skeleton diagram for the vertex V_j into a series of perturbative diagrams using (31), the leading loop order of the new set of diagrams is greater than or equal to the leading loop order of the original set.

item 2: If we include fictitious vertices V_j^0 for $5 \leq j \leq n$, we can convert skeleton diagrams to perturbative diagrams using (31), or perturbative diagrams to skeleton diagrams using (34), and the leading loop order of the new set of diagrams is equal to the leading loop order of the original set.

We illustrate these statements with an example. We use L_{pt} to indicate the loop order of the perturbative expansion. Consider the skeleton diagram shown in part (a) of Fig. 2, which is of order $L = 2$. We can expand this diagram as a series of perturbative diagrams using equations of the form (31) which are shown for this example in part (b) of the figure⁶. The leading order term is shown in part (c), and is of order $L_{pt} = 2$. Thus, we have $L = L_{pt} = 2$. Now, consider the result if we set $V_5^0 = 0$, which means we remove the first diagram on the right side of part (b₂). In this case, the leading order term is shown in part (d) and is of order $L_{pt} = 3$. Thus, we see that if the fictitious vertex V_5^0 is set to zero we have $L_{pt} > L$.

⁶ The propagators in the skeleton diagrams in Fig. 2 also have to be expanded to obtain a perturbative diagram. This will produce extra loops that correspond to self-energy corrections. In this paper, we do not introduce notation to distinguish skeleton and perturbative propagators in diagrams.

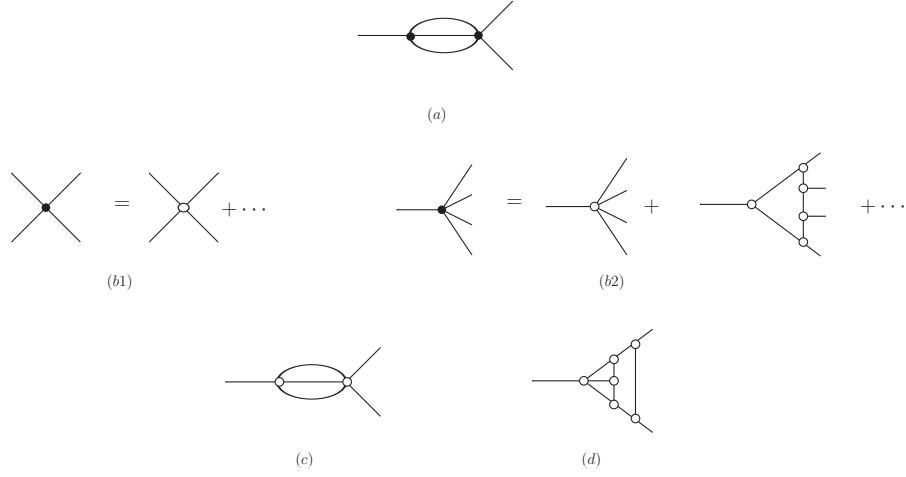


FIG. 2. Diagrams used to explain items 1 and 2.

We consider truncating the n PI effective action at m -loop order⁷. The functional derivative of an m -loop graph with respect to the variational vertex V_j opens $j - 1$ loops. This means that an arbitrary m -loop graph in the effective action which contains the vertex V_j produces a term with $\mathcal{L}[m, j]$ loops in the skeleton expansion of the eom for the vertex V_j , where we define

$$\mathcal{L}[m, j] := m - j + 1. \quad (35)$$

Note that the order of the original m -loop graph in the effective action corresponds to $j = 1$.

Now, we consider the effect of adding an arbitrary $(m + 1)$ loop graph to the skeleton expansion of the m -Loop n PI effective action. This $(m + 1)$ loop graph will produce new contributions to the skeleton expansions of the eom's for each vertex contained in the graph. There are two kinds of contributions:

(1) Taking the functional derivative of this added graph with respect to V_j produces new terms in the skeleton expansions of the V_j eom of order $\mathcal{L}[m + 1, j]$. These new terms contribute at $L = \mathcal{L}[m + 1, j]$ loops in the skeleton expansion and (using item 1) $L_{pt} \geq \mathcal{L}[m + 1, j]$ loops in the perturbative expansion.

(2) We also need to consider lower loop diagrams in the skeleton expansion of V_j of order $\mathcal{L}[m', j]$ ($m' \leq m$), with an arbitrary variational vertex V_k replaced by a term in its eom which was produced by functional differentiation of the $(m + 1)$ loop graph that was added to the effective action. For any k , the new contributions to the vertex V_k from this added graph are of order $\mathcal{L}[m + 1, k]$. The substitution of vertex V_k produces terms of order $L = \mathcal{L}[m', j] + \mathcal{L}[m + 1, k]$ in the skeleton expansion of V_j . Using Eq. (35) and $k_{\max} = m' + 1$ (see Appendix D), we obtain $L \geq \mathcal{L}[m', j] + \mathcal{L}[m + 1, k_{\max}] = \mathcal{L}[m + 1, j]$. Thus, we have shown that these terms also contribute to the eom of the vertex V_j at $L = \mathcal{L}[m + 1, j]$ loops in the skeleton expansion and (using item 1) $L_{pt} \geq \mathcal{L}[m + 1, j]$ loops in the perturbative expansion.

We conclude that if we add an arbitrary $(m + 1)$ loop graph to the skeleton expansion of the m -loop n PI effective action, this graph will produce terms at $\mathcal{L}[m + 1, j]$ loops or higher in both the skeleton and perturbative expansions of the eom for the vertex V_j . Furthermore, we know that

⁷ At m -Loops, the n PI effective action is the same as the $(n + 1)$ PI effective action for $n \geq m$ [29].

without truncation, the expanded effective action and equations of motion for the vertices V_j must exactly match the 1PI perturbative expansion. The conclusion is

item 3: The m -Loop n PI effective action produces all terms in the perturbative expansions of the effective action and the equations of motion for the vertices V_j up to $L_{pt} = \mathcal{L}[m, j]$ loops.

Equivalently, the vertex functions have the correct crossing symmetry to $L_{pt} = \mathcal{L}[m, j]$ loops. We say that the variational vertex functions respect crossing symmetry to the “truncation order.”

Now we consider the Schwinger-Dyson equations, which form an infinite hierarchy of coupled nonlinear integral equations. They have the form

$$V_j^{sd} = V_j^0 + \text{fcn}_j^{sd}[V_l^0, V_k^{sd}]. \quad (36)$$

Although the structure of the sd equations is very different from the eom, when we truncate the sd equations by setting $V_{m+k}^{sd} = V_{m+k}^0$ for $k \geq 1$, the vertex V_j^{sd} also matches the perturbative expansion up to $L_{pt} = \mathcal{L}[m, j]$ loops [31].

If we truncate at some given number of loops, the most general effective action is obtained by considering the same number of variational vertices (see footnote 7). For this reason, from this point on, we consider only $m = n$. Using item 3, we have that

item 4: The perturbative expansions of the n -loop n PI eom’s and the sd equations truncated by setting $V_{n+k}^{sd} = V_{n+k}^0$ for $k \geq 1$ both match the perturbative expansion obtained from the 1PI effective action, and therefore each other, to order $L_{pt} = \mathcal{L}[n, j]$.

We can formally write Eq. (36) as

$$\begin{aligned} V_j^{sd} &= V_j^0 + \text{fcn}_j'[V_l^0, V_k^{sd}] + I_j[V_l^0, V_k^{sd}], \\ I_j[V_l^0, V_k^{sd}] &:= \text{fcn}_j^{sd}[V_l^0, V_k^{sd}] - \text{fcn}_j'[V_l^0, V_k^{sd}]. \end{aligned} \quad (37)$$

We can rewrite $I_j[V_l^0, V_k^{sd}]$ as

$$I_j[V_l^0, V_k^{sd}] = \text{fcn}_j[V_k^{sd}] + \text{extra}, \quad (38)$$

where the functional $\text{fcn}_j[V_k^{sd}]$ can be taken to be the same functional as in (31), since the extra term is defined to absorb any leftovers. Comparing (31) and (37) and using item 4, it is clear that $\text{fcn}_j[V_k]$ and $I_j[V_l^0, V_k^{sd}]$ must match each other in the perturbative expansion to order $L_{pt} = \mathcal{L}[n, j]$. Therefore, we know that the extra term is of order $L_{pt} = \mathcal{L}[n, j] + 1$. Using item 2, the extra term can be rewritten as a series of skeleton diagrams of order $L = \mathcal{L}[n, j] + 1$. Thus, we have shown

item 5: The sd equations can be rearranged to have the same form as the n PI eom’s, plus additional terms of order $L = \mathcal{L}[n, j] + 1$ in the skeleton expansion.

In the next section, we use the result in item 5 to calculate the effective action, without taking a Legendre transform. We emphasize that the proof of this result depends on the use of fictitious bare vertices V_j^0 for $5 \leq j \leq n$. Specifically, items 1, 3, and 4 are true with or without fictitious vertices, but items 2 and 5 are only true when these vertices are included.

V. A NEW APPROACH TO THE CALCULATION OF THE EFFECTIVE ACTION

In this section, we explain the technique of a new approach to calculate (the interacting part of) the n -Loop n PI effective action. The basic idea is to calculate the sd equations, using standard

techniques (see Refs. [33–35]), and then exploit the fact that they can be re-arranged to have the same form as the n PI equations of motion, up to the truncation order (see Sec. IV). One joins the legs of each graph in the rearranged sd equations, to get the structure of the graphs in the effective action. It is clear that this procedure will produce all of the graphs in the effective action, at a given order. The trick is to obtain the correct symmetry factor. In order to see how this can be done, consider starting from a known result for the effective action Φ^{int} , taking derivatives of each graph with respect to each variational vertex, and trying to reconstruct the effective action by joining the legs in each of these eom's. There are two potential difficulties:

(1) A given graph in the effective action will produce contributions to the eom's of each vertex it contains. In order to produce the correct symmetry factor when joining legs, we must drop the corresponding contribution in all but one eom, which we take to be the eom for the largest vertex present. For example, the TARGET graph (see Fig. 4) gives a contribution to the eom of the vertices V_3 and V_4 . We drop the contribution to the V_3 eom and recover the TARGET graph by joining the legs of the contribution to the V_4 eom. If we did not drop contributions to the V_3 eom from the TARGET graph, we would produce unwanted copies of the TARGET graph when we joined the legs in the graphs in the full V_3 eom.

(2) If the largest vertex in a given diagram in the effective action appears more than once, the graph that is produced by joining the legs will have a symmetry factor that is too large by a factor equal to the number of times the vertex appears. For example, consider the LOOPY graph (see Fig. 4). The largest vertex is V_4 which appears 3 times. If we join the legs on the contributions of the LOOPY graph to the V_4 eom, we recover the LOOPY graph, but with a symmetry factor which is 3 times too big.

For any diagram in the equation of motion for the largest vertex V_j , the correct symmetry factor for the contribution to the effective action that we get by joining legs is

$$S[j] = s(1/v_j)(1/j!), \quad (39)$$

where s is the numerical factor in front of the diagram in the eom, and $v_j - 1$ is the number of times the vertex V_j appears in this diagram.

We give two examples of how to use this formula. In the TARGET graph, the largest vertex is V_4 which appears only once, and there are three contributions to the eom for the vertex V_4 , all of which have $s = 1$ and $v_4 - 1 = 0$. Joining legs and using (39) we recover the TARGET graph with symmetry factor $3 \cdot (1) \cdot (1/4!) = 1/8$ (see Fig. 4). In the LOOPY diagram, there are 3 contributions to the eom for the vertex V_4 (which correspond to the s , t , and u channels), all of which have $s = 1/2$ and $v_4 - 1 = 2$. Joining legs and using (39), we recover the LOOPY graph with symmetry factor $3/2 \cdot (1/3) \cdot (1/4!) = 1/48$ (see Fig. 4).

The complete set of rules to generate the interacting part of the n -Loop n PI effective action from the sd equations is given below. In Secs. VI and VII, we describe in detail how the procedure works for the 4-loop 4PI effective action and the 5-loop 5PI effective action.

Step 1: In the classical action, include bare vertices V_j^0 for $3 \leq j \leq n$.

Step 2: Using this new classical action, derive Φ^0 and the sd equations for the vertices V_j for $3 \leq j \leq n$, using standard techniques.

Step 3: Extract from Φ^0 the functions $\text{fcn}'_j[V_l^0, V_k^{sd}]$ which are defined in (30). Once these functions have been obtained, set the fictitious vertices to zero in Φ^0 (and thus remove the nonrenormalizable interactions). The resulting expression for Φ^0 is the same for all n PI effective actions with $n \geq 4$.

Step 4: Rearrange (36) in the form (from this point on, we suppress the superscript “ sd ” on vertices):

$$V_j^0 = V_j - \text{fcn}_{j^0}^{sd}[V_l^0, V_k]. \quad (40)$$

Following the procedure described below, use (40) to remove the bare vertices in the functionals $I_j[V_l^0, V_k]$ defined in (37) for $j = n, n-1, \dots, 3$.

Level 1: Use (40) to remove bare vertices in I_n until all terms with $\mathcal{L}[n, n] := 1$ loop contain no bare vertices. Drop terms in I_n with more than $\mathcal{L}[n, n]$ loops and terms containing V_k with $k \geq n+1$ (because these vertices do not contribute to the n PI effective action). Join the legs of the remaining terms and calculate the symmetry factor $S[n]$ using (39).

Level 2: Use (40) to remove bare vertices in I_{n-1} until all terms with $\mathcal{L}[n, n-1] := 2$ Loops contain no bare vertices. Drop terms in I_{n-1} with more than $\mathcal{L}[n, n-1]$ loops and terms containing V_k with $k \geq n$. Join the legs of the remaining terms and calculate the symmetry factor $S[n-1]$ using (39).

\vdots

Level j : Use (40) to remove bare vertices in I_{n-j+1} until all terms with $\mathcal{L}[n, n-j+1]$ Loops contain no bare vertices. Drop terms in I_{n-j+1} with more than $\mathcal{L}[n, n-j+1]$ loops and terms containing V_k with $k \geq n-j+2$. Join the legs of the remaining terms and calculate the symmetry factor $S[n-j+1]$ using (39).

\vdots

Level $n-2$: Use (40) to remove bare vertices in I_3 until all terms with $\mathcal{L}[n, 3] := n-2$ Loops contain no bare vertices. Drop terms in I_3 with more than $\mathcal{L}[n, 3]$ loops and terms containing V_k with $k \geq 4$. Join the legs of the remaining terms and calculate the symmetry factor $S[3]$ using (39).

Step 5: Add the basketball diagrams with two proper vertices V_j for $3 \leq j \leq n$. The symmetry factor for each graph is $-1/(2(j!))$.

VI. EXAMPLE OF 4-LOOP 4PI EFFECTIVE ACTION.

In this section, we calculate the 4-Loop 4PI effective action and verify that our technique produces the known result [12], which is reproduced in Figs. 3 and 4 for convenience.

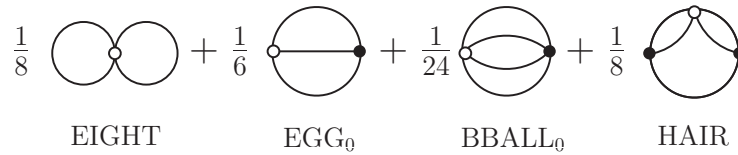


FIG. 3. Φ^0 for a theory with bare vertices V_3^0 and V_4^0 .

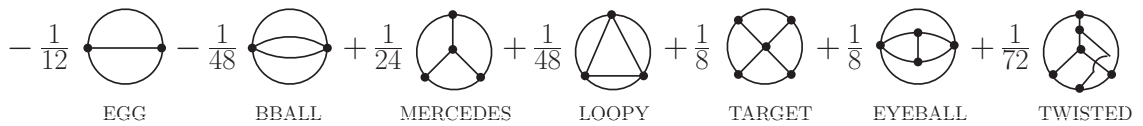


FIG. 4. 4-Loop diagrams contributing to Φ^{int} .

We follow the procedure outlined in the previous section.

Step 1: Start with a classical action that includes bare 3-point and 4-point vertices: V_3^0 and V_4^0 .

Step 2: Calculate Φ^0 and the sd equations using this action. The sd equations for V_3 and V_4 are reproduced from [31] in Figs. 5 and 6.

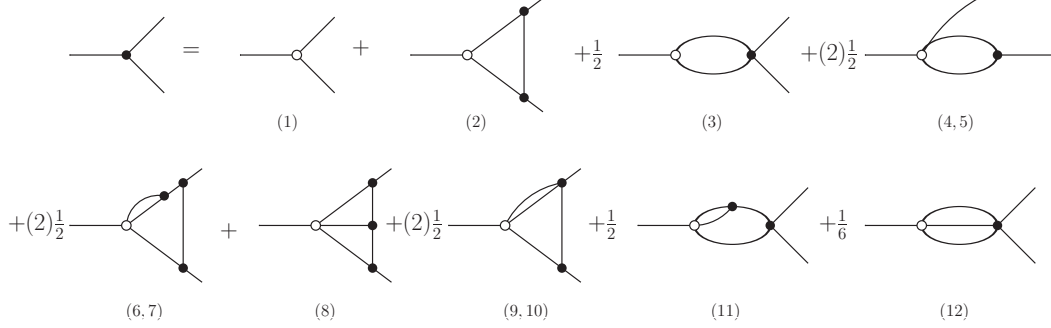


FIG. 5. Schwinger-Dyson equation for the 3-point vertex with V_3^0 and V_4^0 .

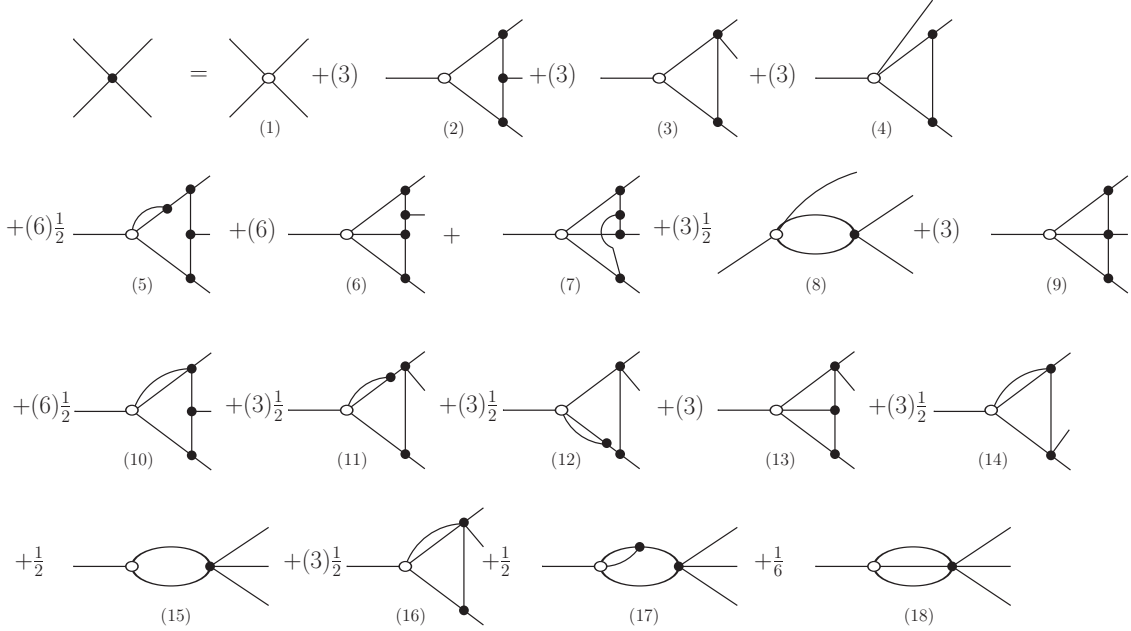


FIG. 6. Schwinger-Dyson equation for the 4-point vertex with V_3^0 and V_4^0 .

Step 3: Extract $\text{fcn}'_3[V_l^0, V_k]$ and $\text{fcn}'_4[V_l^0, V_k]$. The result for $\text{fcn}'_3[V_l^0, V_k]$ is shown in Fig. 7 and $\text{fcn}'_4[V_l^0, V_k] = 0$.

$$\text{fcn}'_3 = (3)\frac{1}{2} \text{ --- } \text{bubble} \text{ ---}$$

FIG. 7. The result for $\text{fcn}'_3[V_l^0, V_k]$. Joining the legs produces the HAIR graph, and calculating the symmetry factor using Eq. (39) gives $(3/2)(1/2)1/3! = 1/8$, which agrees with Fig. 3.

Step 4:

Level 1: We want to obtain a 1-Loop expression for I_4 that does not contain bare vertices. Since $\text{fcn}'_4 = 0$, we simply take the 1-loop diagrams in Fig. 6 and set $V_j^0 = V_j$ and $V_{j \geq 5} = 0$. The three graphs that are produced are shown in Fig. 8. The numbers in brackets under each diagram indicate the corresponding diagrams in the sd equation. For example, the first diagram in Fig. 8 comes from the graph marked (2) in Fig. 6 with $V_3^0 = V_3$. Joining legs, the three diagrams in Fig. 8 produce, respectively, the TARGET, EYEBALL, and LOOPY topologies. We calculate the symmetry factors for each graph using (39). For the three graphs in Fig. 8 we have $v_4 = 1$, $v_4 = 2$, and $v_4 = 3$. The symmetry factors are $3(1)(1/4!) = 1/8$, $6(1/2)(1/4!) = 1/8$, and $3/2(1/3)(1/4!) = 1/48$, which reproduces the result in Fig. 4 for the TARGET, EYEBALL, and LOOPY graphs.

$$I_4 = (3) \text{---} \text{---} \text{---} + (6) \text{---} \text{---} \text{---} + (3)\frac{1}{2} \text{---} \text{---} \text{---} + \dots$$

(2) (3, 4) (8)

FIG. 8. The 1-loop terms in I_4 with bare vertices removed. The numbers in brackets under each diagram indicate the corresponding diagrams in the sd equation (see Fig. 6).

Level 2: We want to obtain an expression for I_3 that does not contain bare vertices at the 2-Loop level. We start with the 2-Loop diagrams in Fig. 5 and subtract fcn'_3 (see Fig. 7). We set $V_{j \geq 4} = 0$ (recall that vertices with $j \geq 5$ are set to zero because they are not part of the 4PI effective action, and vertices V_4 are set to zero to avoid double counting contributions that were obtained in Level 1 above). This produces graphs that we refer to as “explicit 1-loop” and “explicit 2-loop”. After the bare vertices are removed using (40), the explicit 1-loop graphs will produce 2-loop contributions.

explicit 2-loop: We remove bare vertices in the explicit 2-loop graphs by setting $V_j^0 = V_j$. Using $V_{j \geq 4} = 0$, all 2-loop graphs drop out.

explicit 1-loop: The explicit 1-loop contributions to I_3 with $V_{j \geq 4} = 0$ are shown in Fig. 9. We remove bare vertices using (40), iterated so that there are no bare vertices in the 1-Loop terms. These iterated expressions with $V_{j \geq 4} = 0$ are shown in Fig. 10. The result of substituting Fig. 10 into Fig. 9 is shown in Fig. 11. Note that the 2 graphs which would produce a 4PR contribution to the effective action cancel identically. The final step is to join the legs and calculate the symmetry factor using (39). The surviving diagram from the top line in Fig. 11 produces the MERCEDES graph, and the survivor from the second line produces the TWISTED graph (see Fig. 4).

$$I_3 = \text{---} \text{---} \text{---} - \frac{1}{2} \text{---} \text{---} \text{---}$$

(2) (4, 5) - fcn'_3

FIG. 9. The 1-loop terms in I_3 . The numbers in brackets under each diagram indicate the corresponding graph in the sd equation in Fig. 5, and fcn'_3 is shown in Fig. 7.

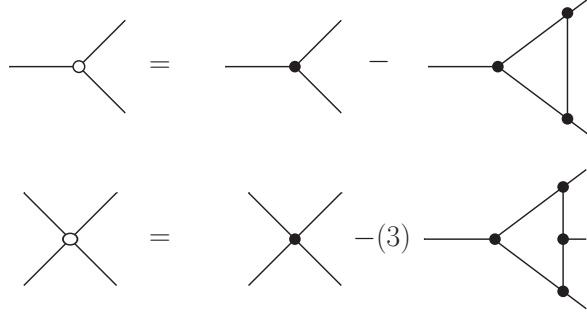


FIG. 10. The result of iterating Eq. (40) so that 1-loop graphs do not contain bare vertices.

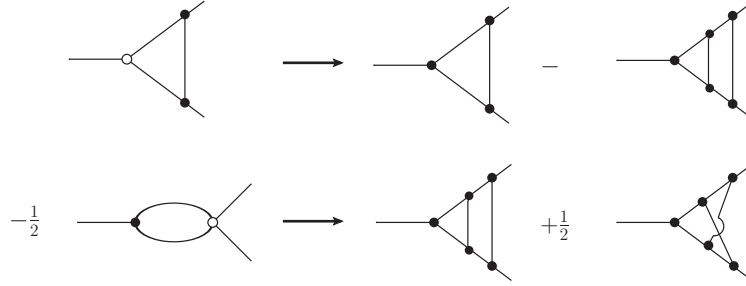


FIG. 11. The diagram obtained by substituting Fig. 10 into Fig. 9.

Step 5: Add the basketball diagrams which are the EGG and BBALL diagrams (see Fig. 4).

VII. 5-LOOP 5PI EFFECTIVE ACTION.

For $n \geq 5$, we need to introduce fictitious bare vertices. We illustrate the role of these vertices by describing the 5-loop 5PI calculation. Some details are left to Appendix A. The result of the calculation is known [31]. For convenience, we reproduce in Fig. 12 the 5-loop diagrams.

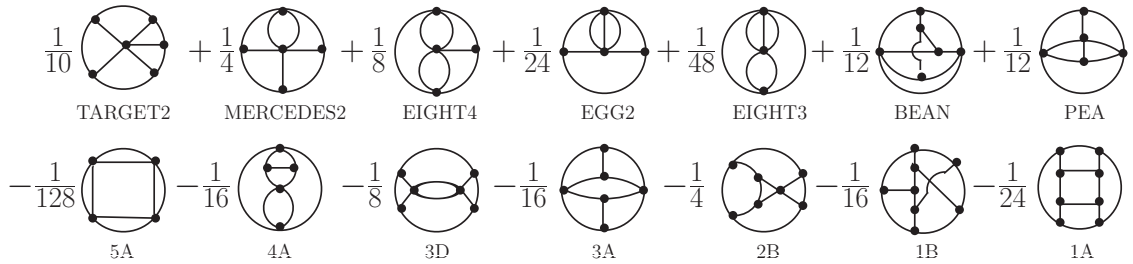


FIG. 12. 5-loop diagrams contributing to Φ^{int} for the 5PI effective action.

We follow the steps in Sec. V.

Step 1: We include bare vertices V_3^0 , V_4^0 , and V_5^0 in the Lagrangian.

Step 2: We calculate Φ^0 and the sd equations for the vertices V_j , $3 \leq j \leq 5$. The result for Φ^0 is given in Fig. 3 and the first line of Fig. 17, excluding the basketball diagram with the vertex V_6^0 .

The fictitious vertices produce many contributions to the sd equations, but not all are needed to calculate the 5-loop 5PI effective action.

In Step 4, we will need to calculate I_5 to 1-Loop level, which means we only need 1-Loop terms in the sd equation for V_5 . These 1-loop diagrams are the first 10 graphs on the right side of Fig. 13.

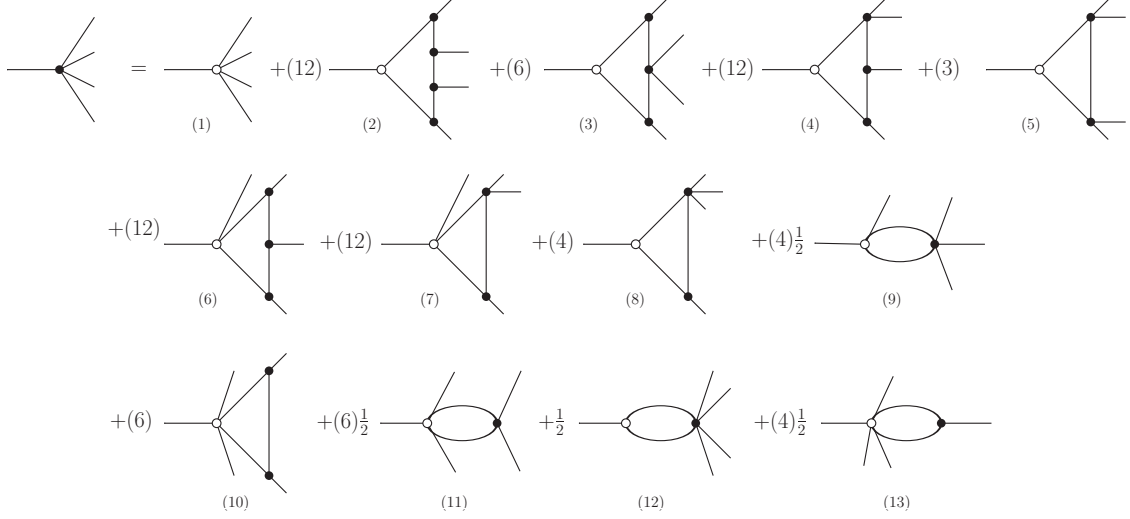


FIG. 13. 1-Loop terms in the Schwinger-Dyson equation for the 5-point vertex with V_j^0 for $3 \leq j \leq 6$.

In addition, the sd equations for the vertices V_3 and V_4 in Figs. 5 and 6 receive extra contributions from diagrams with the vertex V_5^0 . For V_4 , we need 1-loop diagrams with $V_{j \geq 5} = 0$ and 2-loop diagrams with $V_j^0 = V_j$ and $V_{j \geq 5} = 0$. For V_3 , we need 2-Loop diagrams with $V_{j \geq 4} = 0$ and 3-loop diagrams with $V_j^0 = V_j$ and $V_{j \geq 4} = 0$. These extra diagrams are shown in Fig. 14.

$$\begin{aligned}
 V_3^{extra} &= \frac{1}{2} \text{ (diagram 1) } + (2)\frac{1}{2} \text{ (diagram 2) } + \frac{1}{4} \text{ (diagram 3) } + \dots \\
 V_4^{extra} &= (3)\frac{1}{2} \text{ (diagram 4) } + \dots
 \end{aligned}$$

FIG. 14. Some extra terms in the sd equations for V_3 and V_4 containing V_5^0 .

Step 3: From Φ^0 , we extract fcn'_i with $i = 3$ and 4. The results are shown in Fig. 15. We have $\text{fcn}'_5 = 0$ at the 5-Loop 5PI level.

$$\begin{aligned} \text{fcn}'_3 &= (3)_{\frac{1}{2}} \text{---} \text{---} \text{---} + (3)_{\frac{1}{6}} \text{---} \text{---} \text{---} + (3)_{\frac{1}{2}} \text{---} \text{---} \text{---} + (3)_{\frac{1}{4}} \text{---} \text{---} \text{---} + \frac{1}{2} \text{---} \text{---} \text{---} \\ \text{fcn}'_4 &= (4)_{\frac{1}{2}} \text{---} \text{---} \text{---} \end{aligned}$$

FIG. 15. Results for fcn'_3 and fcn'_4 .**Step 4:**

Level 1: We construct I_5 at the 1-loop level. The 1-loop terms in the sd equation are shown in Fig. 13, and $\text{fcn}'_5 = 0$. We replace bare vertices with proper ones $V_j^0 = V_j$ and set $V_{j \geq 6} = 0$, which removes the last two diagrams. The surviving terms are shown in Fig. 16.

$$I_5 = (12) \text{---} \text{---} \text{---} + (30) \text{---} \text{---} \text{---} + (15) \text{---} \text{---} \text{---} + (10) \text{---} \text{---} \text{---} + (10)_{\frac{1}{2}} \text{---} \text{---} \text{---} + \dots$$

(2) (3, 4, 6) (5, 7) (8, 10) (9, 11)

FIG. 16. One-loop contributions to I_5 . The numbers in brackets under each diagram indicate the corresponding graph in the sd equation in Fig. 13.

The final step is to join the legs and calculate the symmetry factor from (39). The fourth graph has $v_5 = 2$ and $S = 10 \cdot (1/2) \cdot (1/5!) = 1/24$, which reproduces EGG2, and the fifth has $v_5 = 2$ and $S = 5 \cdot (1/2) \cdot (1/5!) = 1/48$, which reproduces EIGHT3 (see Fig. 12). Note that the graphs marked (10) and (11) in Fig. 13, which contain the vertex V_5^0 , are needed to obtain these results. This is an example of the role of the fictitious bare vertices. The first three graphs in Fig. 16 produce the TARGET2, MERCEDES2, and EIGHT4 graphs, respectively, (see Fig. 12).

Levels 2 and 3: We need to construct I_4 at the 2-Loop level and I_3 at the 3-Loop level. Some details of the calculation are given in Appendix A.

Step 5: We add the 2-, 3-, and 4-loop basketballs.

Combining all pieces, we reproduce the 5-Loop 5PI effective action, which was obtained through a much more lengthy calculation in [31], using Legendre transforms.

VIII. RESULT FOR 6-LOOP 6PI

The 6-Loop 6PI effective action can be calculated using the same method.

Step 1: We include bare vertices V_j^0 for $3 \leq j \leq 6$ in the Lagrangian.

Step 2: The additional terms in Φ^0 and the sd equation for the self-energy which contain V_5^0 and V_6^0 are shown in Figs. 17 and 18, respectively.

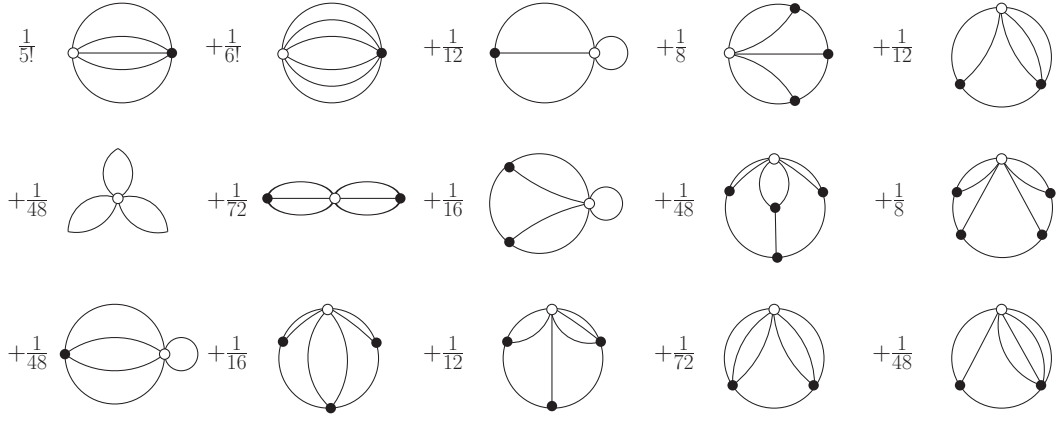


FIG. 17. 5-Loop contributions to Φ^0 that contain the bare vertices V_5^0 and V_6^0 .

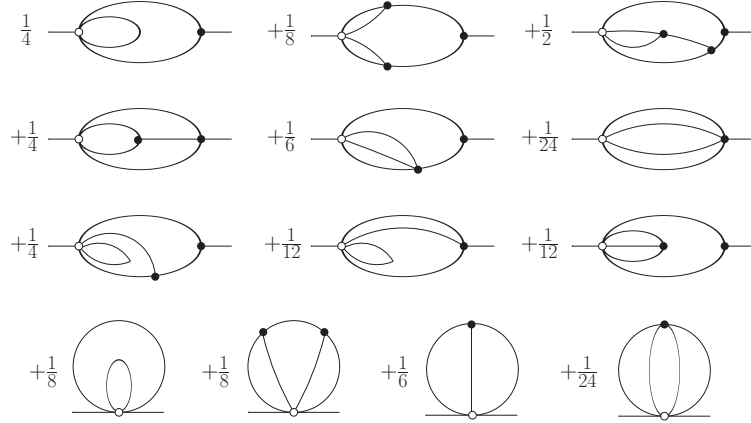
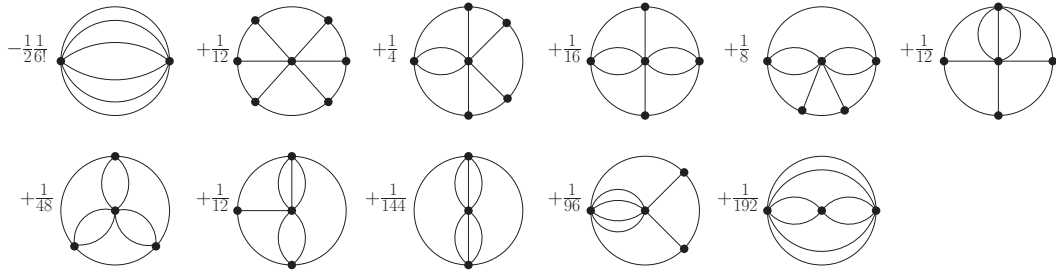
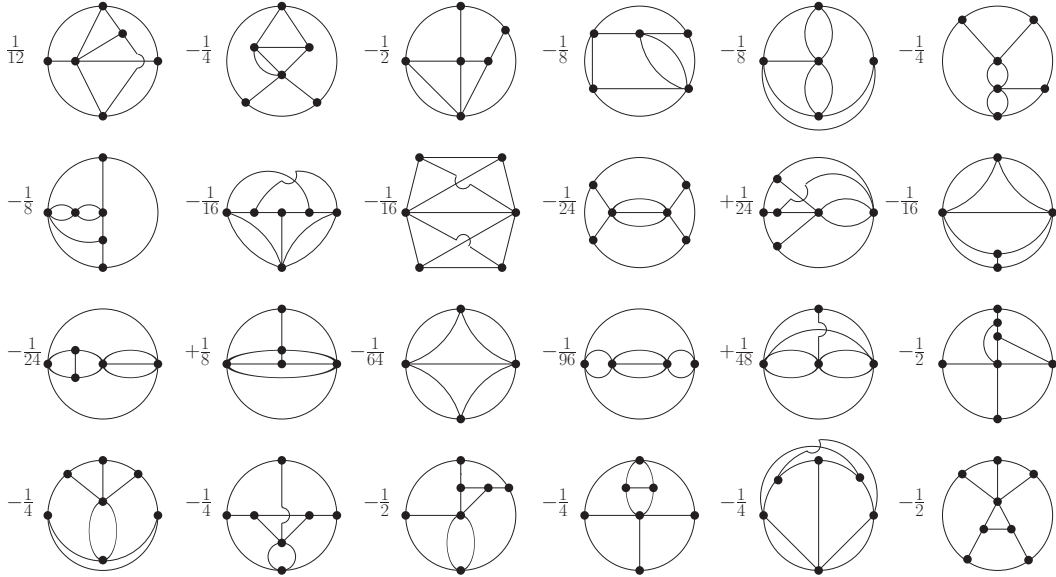


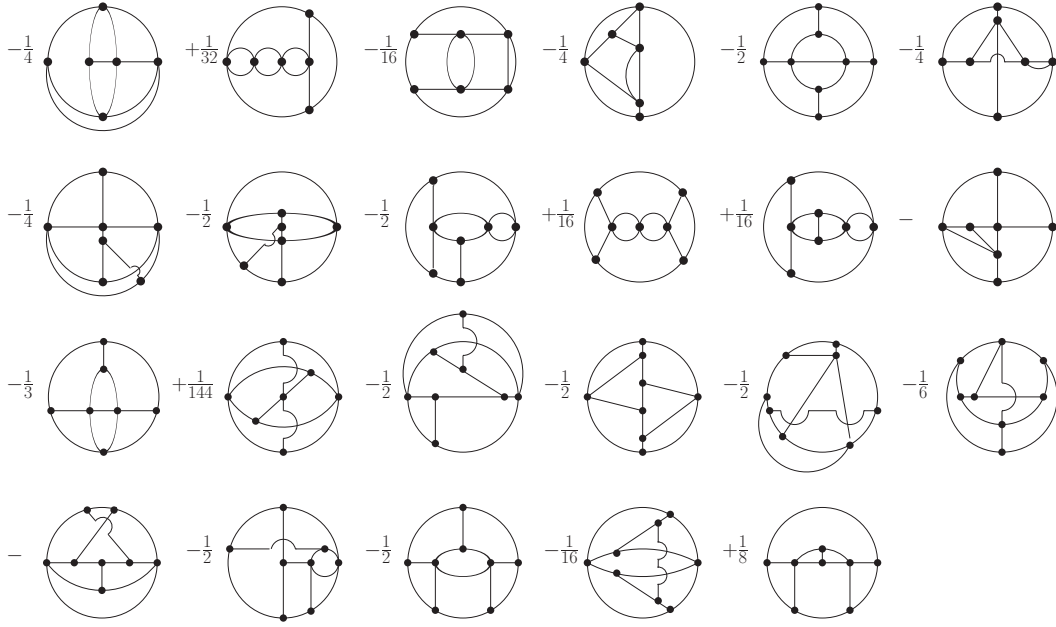
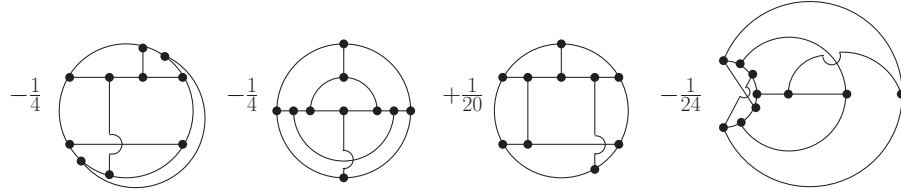
FIG. 18. 3-Loop contributions to the sd equation for Π from terms with V_5^0 and V_6^0 .

Using these expressions, it is straightforward to generate the corresponding results for the sd equations for V_j for $3 \leq j \leq 6$. After combining permutations of external indices, the sd equation for the vertex V_6 contains 20 1-loop terms, the equation for V_5 contains 12 1-loop terms, and 62 2-loop terms, the equation for V_4 contains 7 1-loop terms, 27 2-loop terms, and 88 3-loop terms, and the equation for V_3 contains 5 1-loop terms, 12 2-loop terms, 31 3-loop terms, and 49 4-loop terms⁸.

It is straightforward to follow the procedure outlined in Sec. V and illustrated in Secs. VI and VII. The calculation can be done using Mathematica. We give only the result below. Diagrams with highest V_j equal to V_6 , V_5 , V_4 , and V_3 are shown in Figs. 19, 20, 21 and 22, respectively.

⁸ The 3-loop contributions to the V_4 equation are not needed since they all contain V_5^0 or V_6^0 and thus drop out when we set $V_j^0 = V_j$ and $V_j = 0$ for $j \geq 5$. Similarly, the 4-loop contributions to the V_3 equation are not needed since they all contain V_6^0 and drop out when we set $V_j^0 = V_j$ and $V_j = 0$ for $j \geq 4$.

FIG. 19. 6-loop diagrams with highest vertex V_6 and the basketball with V_6 .FIG. 20. 6-loop diagrams with highest vertex V_5 .

FIG. 21. 6-loop diagrams with highest vertex V_4 .FIG. 22. 6-loop diagrams with highest vertex V_3 .

IX. CONCLUSIONS

The n PI effective action at higher orders is a potentially useful tool to study nonequilibrium systems, like the quark gluon plasma and the early Universe. In this paper, we have introduced a new method to calculate the n -Loop n PI effective action which does not require a Legendre transform and makes it possible to calculate the effective action at higher orders than was previously possible. The key to our method is the introduction of a set of fictitious bare vertices which are used only as an organizational trick. Using these fictitious vertices, we have shown that the n PI equations of motion and Schwinger-Dyson equations are equivalent to the order at which the truncated theory respects the symmetries of the original theory. This result makes it possible to systematically construct the n -Loop n PI effective action directly from the sd equations, which are relatively easy to calculate. The known results for the n -Loop n PI effective action with $n = 4$ and $n = 5$ can be obtained with comparatively little effort using our method, which provides a check of the procedure. In addition, we have used the technique to calculate the 6-Loop 6PI effective action, which is essentially impossible to obtain using the standard method employing Legendre transforms.

We remove bare vertices using (40) iterated to 1-Loop order with $V_{j \geq 5} = 0$. The equations we obtain from (40) are shown in Fig. 24, and the 2-loop diagrams obtained by substituting these expressions into the explicit 1-loop diagrams in I_4 are shown on the right side of Fig. 23. The 1-loop diagrams can be ignored since they are, by construction, the same as in Fig. 8, and therefore produce the TARGET, EYEBALL, and LOOPY diagrams as in Sec. VI.

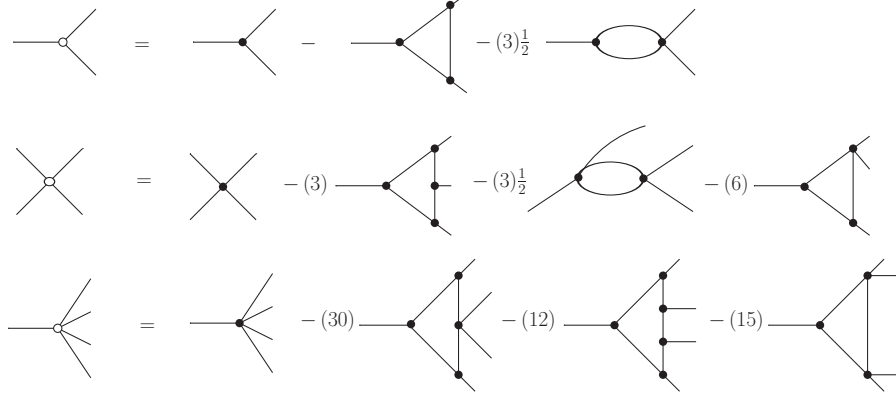


FIG. 24. The result obtained from (40) which will be used to replace the bare vertices in the diagrams on the left side of Fig. 23.

We add the diagrams on the right side of Fig. 23 and the explicit 2-loop terms [diagrams (5), (6), (7), (9), (10), (11), (12), (13), and (14) in Fig. 6 with $V_j^0 = V_j$]. The terms that cancel are $i_1 + i_2$, $j_1 + j_2$, $(5) + k$, $l_1 + l_2$, $m_1 + m_2$, $(11) + (12) + n_1 + n_2$, $o_1 + o_2$, $(6) + p_1 + p_2$, $(10) + q$, $r_1 + r_2$, $(13) + s_1 + s_2$, $(14) + t$. The survivors are A, $B_1 + B_2$, C, $D_1 + D_2$, E, F, $(7) + G$, $(9) + H$ and are shown in Fig. 25⁹.

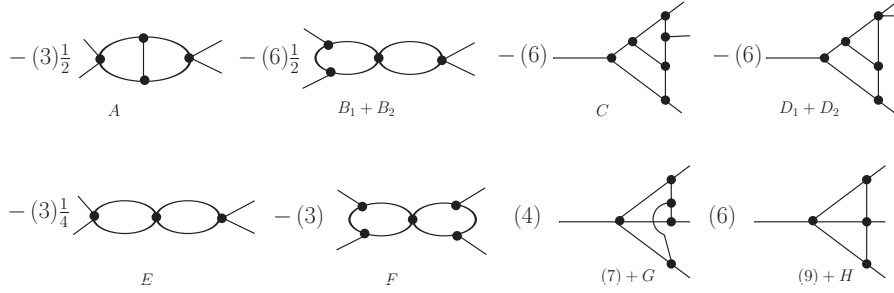


FIG. 25. 2-loop contributions to I_4 . The labels under the diagrams indicate the corresponding pieces of Figs. 23 and 6.

The last step is to join the legs of each graph in Fig. 25 and calculate the symmetry factor using (39). The first two diagrams in Fig. 25 both give the same contribution to the effective action: the diagram 4A in Fig. 12. For the first graph, the symmetry factor is $-3/2 \cdot (1/3) \cdot (1/4!) = -1/48$, and for the second graph we have $-3 \cdot (1/3) \cdot (1/4!) = -1/24$. Summing these factors, we obtain $-1/16$, which agrees with Fig. 12. The last 6 diagrams give, in order, the graphs labeled 2B, 3D, 5A, 3A, BEAN, and PEA in Fig. 12.

⁹ In Fig. 24, the permutations of external legs are not symmetric. The numerical factor in brackets in front of each diagram indicates the number of permutations only. However, for every set of graphs that cancels, each permutation of external legs cancels individually. For sets of graphs that do not cancel, every possible permutation of external legs is produced. Both of these results are guaranteed by the proof in Sec. IV.

Next, we construct I_3 at the 3-Loop level.

I_3 is given by the terms (2,4,5,6,7,8) in Fig. 5, plus the additional terms in Fig. 14 which contain the bare vertex V_5^0 , minus the terms in fcn'_3 in Fig. 15, with $V_4=0$. We use (40) to iterate the sd equations to 2-Loop level, setting $V_{j \geq 4} = 0$. This procedure produces the results in Fig. 24 with $V_4 = 0$, plus the 2-loop diagrams in Fig. 26. As mentioned in the discussion about Fig. 23, we do not need to separate graphs that correspond to different permutations of external legs, since we will join legs to obtain the corresponding contribution to the effective action. In Fig. 26, we do not indicate contributions to the numerical factor from permutations of external legs.

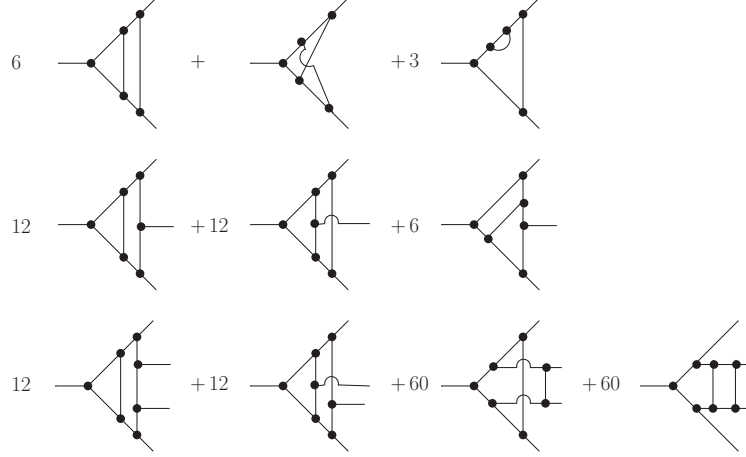


FIG. 26. 2-loop contributions to V_3 , V_4 , and V_5 obtained from (40) with $V_{j \geq 4} = 0$.

explicit 3-loop: Setting $V_j^0 = V_j$ and $V_{j \geq 4} = 0$, there are no surviving terms in I_3 .

explicit 2-loop: We take terms in I_3 that are explicitly 2-loop and set $V_{j \geq 4} = 0$. Then, we replace bare vertices using the 1-Loop expressions in Fig. 24.

explicit 1-loop: We take terms in I_3 that are explicitly 1-loop and set $V_{j \geq 4} = 0$. Then, we replace bare vertices using the 2-Loop expressions in Figs. 24 and 26.

The 1- and 2-loop graphs that are produced by this procedure can be ignored, since they reproduce the MERCEDES and TWISTED diagrams obtained previously (Sec. VI). After all cancellations have been identified, the surviving 3-loop diagrams are shown in Fig. 27. Joining the legs produces the graphs labeled 1A and 1B in Fig. 12.

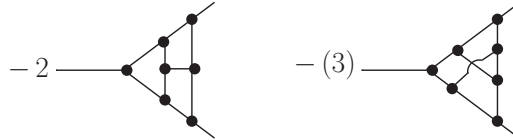


FIG. 27. 3-loop diagrams in I_3 .

Appendix B: Formula for disconnected pieces of correlation functions

We give a general expression for the function χ_j of the form

$$\chi_j = \sum_k a^{[k]} \prod_{i=1}^{j-1} (V_i^c)^{f_i^{[k]}}. \quad (\text{B1})$$

The index k represents different solutions to the equation

$$\sum_{i=1}^{j-1} i f_i^{[k]} = j, \quad j \geq 3. \quad (\text{B2})$$

The symmetry factor $a^{[k]}$ for each term is given by

$$a^{[k]} = \prod_{i=1}^{j-1} \alpha_i, \quad \alpha_i = \frac{1}{f_i^{[k]}!} \prod_{m=0}^{f_i^{[k]}-1} C_{j'_i-m}^i, \quad j'_i = j - \sum_{l=0}^{i-1} l f_l^{[k]}, \quad (\text{B3})$$

where we have defined $C_m^j \equiv m!/(j!(m-j)!)$. We illustrate this formula with an example. For $j = 5$, the possible solutions to (B2) are

$$\begin{aligned} k=1: & \quad f_1^{[1]} = 5, \quad f_2^{[1]} = 0, \quad f_3^{[1]} = 0, \quad f_4^{[1]} = 0, \\ k=2: & \quad f_1^{[2]} = 3, \quad f_2^{[2]} = 1, \quad f_3^{[2]} = 0, \quad f_4^{[2]} = 0, \\ k=3: & \quad f_1^{[3]} = 1, \quad f_2^{[3]} = 2, \quad f_3^{[3]} = 0, \quad f_4^{[3]} = 0, \\ k=4: & \quad f_1^{[4]} = 2, \quad f_2^{[4]} = 0, \quad f_3^{[4]} = 1, \quad f_4^{[4]} = 0, \\ k=5: & \quad f_1^{[5]} = 1, \quad f_2^{[5]} = 0, \quad f_3^{[5]} = 0, \quad f_4^{[5]} = 1, \\ k=6: & \quad f_1^{[6]} = 0, \quad f_2^{[6]} = 1, \quad f_3^{[6]} = 1, \quad f_4^{[6]} = 0. \end{aligned} \quad (\text{B4})$$

- For the $k = 6$ solution in (B4), there are two nonzero values $f_2^{[6]} = 1$ and $f_3^{[6]} = 1$, which means $a^{[6]} = \alpha_2 \cdot \alpha_3$.
- For the α_2 term, we have $j'_2 = 5 - f_1^{[6]} = 5$ and $C_{5-2m}^2 = (5-2m)!/(2!(3-2m)!)$. The limits on the m product are 0 to $f_2^{[6]} - 1 = 0$, and therefore $m = 0$ is the only term that contributes. The $m = 0$ term is $C_5^2 = 10$. We multiply by a factor $1/f_2^{[6]}! = 1$ and obtain $\alpha_2 = 10$.
- For the α_3 term, we have $j'_3 = 5 - f_1^{[6]} - 2f_2^{[6]} = 3$ and $C_{3-3m}^3 = (3-3m)!/(3!(-3m)!)$. The limits on the m product are 0 to $f_3^{[6]} - 1 = 0$, and therefore $m = 0$ is again the only term that contributes, which gives $C_3^3 = 1$. We multiply by a factor $1/f_3^{[6]}! = 1$ and obtain $\alpha_3 = 1$.
- Multiplying these factors together, the result is $a^{[6]} = \alpha_2 \cdot \alpha_3 = 10 \cdot 1$.
- Substituting into (B1), the contribution to χ_5 from the $k = 6$ solution in (B4) is $10DV_3^c$.

In the same way we calculate the $a^{[k]}$ for $k = 1, 2, 3, 4, 5$. We give a summary of the results.

$$\begin{aligned} k=5: & \quad \alpha_1 = 5, \quad \alpha_4 = 1, \quad a^{[5]} = 5, \\ k=4: & \quad \alpha_1 = 10, \quad \alpha_3 = 1, \quad a^{[4]} = 10, \\ k=3: & \quad \alpha_1 = 5, \quad \alpha_2 = 3, \quad a^{[3]} = 15, \\ k=2: & \quad \alpha_1 = 10, \quad \alpha_2 = 1, \quad a^{[2]} = 10, \\ k=1: & \quad \alpha_1 = 1, \quad a^{[1]} = 1. \end{aligned} \quad (\text{B5})$$

Combining these results, Eq. (14) for $j = 5$ becomes

$$\langle \phi^5 \rangle = V_5^c + (5)V_4^c \phi + (10)V_3^c \phi^2 + (10)V_3^c D + (10)D\phi^3 + (15)D^2\phi + \phi^5. \quad (\text{B6})$$

In Sec. III, we divide the term χ_j into different pieces by defining

$$\chi_j = \chi_j^{(0)} + \chi_j^{(1)} + \chi_j^{(2)} + \chi_j^{(3)}. \quad (\text{B7})$$

We explain this notation below. It is clear that (B2) always has three solutions which we write

$$\begin{aligned} k=1: & \quad f_1^{[1]} = j, \quad f_l^{[1]} = 0, \quad l \geq 2, \\ k=2: & \quad f_1^{[2]} = j-2, \quad f_2^{[2]} = 1, \quad f_l^{[2]} = 0, \quad l \geq 3, \\ k=3: & \quad f_1^{[3]} = j-2d, \quad f_2^{[3]} = d, \quad f_l^{[3]} = 0, \quad l \geq 3 \text{ and } j/2 \geq d \geq 2. \end{aligned} \quad (\text{B8})$$

From (B3), it is easy to see that $a^{[1]} = 1$, $a^{[2]} = C_j^2$, and $a^{[3]} = j!/((j-2d)!d!2^d)$. These three solutions give, respectively,

$$\begin{aligned} \chi_j^{(0)} &= \phi^j \quad \text{for } j \geq 3, \\ \chi_j^{(1)} &= C_j^2 D \phi^{j-2} \quad \text{for } j \geq 3, \\ \chi_j^{(2)} &= \frac{j!}{(j-2d)!d!2^d} D^d \phi^{j-2d} \quad \text{for } j \geq 4 \text{ and } j/2 \geq d \geq 2. \end{aligned} \quad (\text{B9})$$

The term $\chi_j^{(3)}$ is defined to be everything that is not contained in $\chi_j^{(0)} + \chi_j^{(1)} + \chi_j^{(2)}$.

Appendix C: Bare vertex part of the effective action

In this section, we discuss how to calculate the part of the effective action that contains bare vertices. We look at the example $V_{j \geq 5}^{oo} = 0$. Using (4), (5), (13) and (B9) we obtain

$$\begin{aligned} \Gamma_0^{oo} - \sum_{j=3}^4 \frac{i}{j!} \chi_j^{(0)} V_j^{oo} &= S_{cl}, \\ \Gamma_1^{oo} - \sum_{j=3}^4 \frac{i}{j!} \chi_j^{(1)} V_j^{oo} &= \frac{i}{2} \text{Tr} \text{Ln} D^{-1} + \frac{i}{2} \text{Tr} [(D^0)^{-1} D], \\ - \sum_{j=3}^4 \frac{i}{j!} \chi_j^{(2)} V_j^{oo} &= -i\text{EIGHT}, \\ - \sum_{j=3}^4 \frac{i}{j!} \chi_j^{(3)} V_j^{oo} &= -\frac{i}{4!} (4) V_3^c \phi V_4^{oo} = -i\text{EGG}_0^a, \\ - \sum_{j=3}^4 \frac{i}{j!} V_j^c V_j^{oo} &= -\frac{i}{3!} V_3 D^3 V_3^{oo} - \frac{i}{4!} D^4 [V_4 + 3(V_3 D V_3)] V_4^{oo} = -i\text{EGG}_0^b - i\text{BBALL}_0 - i\text{HAIR}. \end{aligned} \quad (\text{C1})$$

The terms in the square bracket in the last line come from rewriting the connected vertex V^c in terms of proper vertices. Adding the EGG contributions, we get the diagram with one effective bare vertex: $\text{EGG}_0^a + \text{EGG}_0^b = \text{EGG}_0[V_3^0, V_3]$. Combining all contributions, we obtain the result for $\Gamma^0[\phi, D, V_j^0, V_k]$ in Eq. (19) with

$$\Phi^0[V_j^0, V_k] = \text{EIGHT} + \text{EGG}_0 + \text{HAIR} + \text{BBALL}_0. \quad (\text{C2})$$

The diagrams denoted EIGHT, EGG₀, HAIR, and BBALL₀ are shown in Fig. 3. Equation (C2) is the usual result for the part of the effective action that contains bare vertices (see, for example, [31]).

It is straightforward to calculate $\Gamma^0[\phi, D, V_j^0, V_k]$ for a theory with fictitious vertices. The classical action will contain additional terms [see Eq. (4)]. The effective bare propagator and effective bare vertices are correspondingly modified [see Eq. (5)]. The 1-loop piece will have the same functional form; the only change is that it will depend on the modified effective bare propagator. All of the graphs in Fig. 3 will be present in the same form; the only change is that they now depend on the modified effective bare vertices. There will also be new contributions to Φ^0 . For the example V_5^{oo} and V_6^{oo} nonzero, the new graphs are shown in Fig. 17.

Appendix D: k_{\max} and basketballs

In this Appendix, we show that in the m -Loop n PI effective action, the largest vertex that appears is $V_{k_{\max}}$ with $k_{\max} = m + 1$, and the vertex V_{m+1} appears only in the m -loop basketball diagram.

Using I for the number of internal lines, E for the number of external legs, and v_k for the number of k -point vertices, the standard topological relations are

$$m = I - \sum_{k=3}^n v_k + 1, \quad 2I + E = \sum_{k=3}^n k v_k. \quad (\text{D1})$$

Eliminating I and setting $E = 0$, we get

$$m = 1 + \sum_{k=3}^{k_{\max}} \left(\frac{1}{2}k - 1 \right) v_k. \quad (\text{D2})$$

Our goal is to find k_{\max} for fixed m . We note that every term in the sum in (D2) is positive.

Case 1: It appears that k_{\max} corresponds to $v_k = 0$ for $k \neq k_{\max}$ and $v_{k_{\max}} = 1$. Substituting into (D2), we obtain $k_{\max} = 2m$. However, diagrams with only one vertex are type 1 tadpoles [see part (b₁) of Fig. 1], and we know that tadpole graphs do not appear in the effective action (see Sec. III).

Case 2: We consider the solution $v_k = 0$ for $k \neq k_{\max}$ and $v_{k_{\max}} = 2$, which corresponds to a m -loop basketball diagram. Substituting into (D2), we obtain $k_{\max} = m + 1$.

Case 3: In order to conclude that $k_{\max} = m + 1$ is the biggest solution for k_{\max} , we must check the case $v_{k_{\max}} = 1$ and $v_k \neq 0$ for some values $k < k_{\max}$. We need to determine maximum number of legs from the vertices $V_{k \neq k_{\max}}$ that are available to connect with the lone $V_{k_{\max}}$ vertex without producing a tadpole graph. It is clear that no vertex can have two legs that connect to each other [to avoid creating a tadpole like the graph shown in part (b₃) of Fig. 1], and each vertex must connect to at least two other vertices [to avoid creating a tadpole like the graph shown in part (b₂) of Fig. 1]. Thus, the maximum number of legs from the vertices $V_{k \neq k_{\max}}$ that can connect to the $V_{k_{\max}}$ vertex is

$$k_{\max} = \sum_{k=3}^{k_{\max}-1} (k v_k - 2 v_k) + 2. \quad (\text{D3})$$

A graph that corresponds to Eq. (D3) is given in Fig. 28. Rearranging (D2) in the form

$$m = 1 + \frac{1}{2} \sum_{k=3}^{k_{\max}-1} \left(k - 2 \right) v_k + \frac{k_{\max}}{2} - 1, \quad (\text{D4})$$

and substituting (D3) into (D4) we obtain $k_{\max} = m + 1$, as in Case 2 above. This result appears to indicate that there is a large set of diagrams of the form shown in Fig. 28, in addition to the m -loop basketball diagram, that contains the vertex $V_{k_{\max}=m+1}$. However, all diagrams of the form shown in Fig. 28 are flower topologies, which we know do not appear in the effective action (see Sec. III).

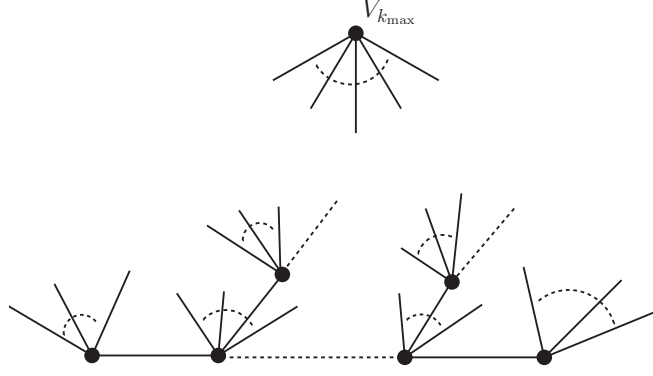


FIG. 28. The maximum number of legs that are available to be connected to $V_{k_{\max}}$.

Since all terms in the sum in (D2) are positive, it is clear that solutions that correspond to $v_{k_{\max}} > 2$, or $v_{k_{\max}} = 2$ and $v_k \neq 0$ for some values $k < k_{\max}$, will produce a smaller value of k_{\max} . We conclude that in the m -Loop n PI effective action, the largest vertex that appears is $V_{k_{\max}}$ with $k_{\max} = m + 1$, and the vertex V_{m+1} appears only in the m -loop basketball diagram.

Appendix E: Equivalence of the eom and sd equation for the self-energy

The equation of motion for the 2-point vertex function obtained from the n -Loop n PI effective action can be rearranged to have the same form as the sd equation, without the use of fictitious vertices. In this Appendix, we prove this result. The sd equation for the 2-point function is shown in Fig. 29.

$$\Pi = \frac{1}{2} \text{(1)} + \frac{1}{2} \text{(2)} + \frac{1}{2} \text{(3)} + \frac{1}{6} \text{(4)}$$

FIG. 29. Schwinger-Dyson equation for the 2-point vertex.

The eom for the 2-point function is obtained from Eq. (33). For the moment, we continue to use the abbreviated notation in which the indices which indicate the coordinates of each leg are suppressed. Using this notation, the eom can be written

$$\Pi = \frac{1}{2} V_4^0 D + 2 \frac{1}{2!} V_3 D^2 V_3^0 + 2 \frac{1}{3!} V_4 D^3 V_4^0 - \sum_{j=3}^n \frac{1}{(j-1)!} V_j D^{j-1} V_j + \sum_i \Pi[\text{diag}^{(i)}]. \quad (\text{E1})$$

The first three terms in this expression come from differentiating the EIGHT, EGG₀, and BBALL₀ diagrams in Φ^0 , respectively, (see Fig. 3). The first sum gives the contributions from the basketball diagrams in Φ^{int} which we will call Π basketballs. The second sum contains contributions from the

HAIR diagram in Φ^0 and all nonbasketball diagrams in Φ^{int} . We can replace one of the vertices in each Π -basketball diagram using Eq. (30). Rewriting (30) as

$$V_j = V_j^0 + \text{fcn}'_j[V_l^0, V_k] + \text{fcn}_j[V_k] =: V_j^0 + \sum_i \text{f}_j[\text{diag}^{(i)}], \quad (\text{E2})$$

we obtain

$$\begin{aligned} \Pi &= \frac{1}{2}V_4^0 D + \frac{1}{2!}V_3 D^2 V_3^0 + \frac{1}{3!}V_4 D^3 V_4^0 + \sum_i \text{EX}^{(i)}, \\ \text{EX}^{(i)} &= - \sum_{j=3}^n \frac{1}{(j-1)!} V_j D^{j-1} \text{f}_j[\text{diag}^{(i)}] + \Pi[\text{diag}^{(i)}]. \end{aligned} \quad (\text{E3})$$

The first three terms on the right side of the first line of (E3) are the diagrams labeled (1), (2), and (4) in Fig. 29. It is straightforward to show that $\text{EX}^{(\text{HAIR})}$ is the diagram labeled (3) in Fig. 29. We show below that $\text{EX}^{(i)}=0$ for any diagram except for the HAIR diagram.

An arbitrary diagram with symmetry factor S , I internal lines, and v_k vertices V_k for $k \geq 3$ can be written

$$\text{diag}^{(i)} = S D^I \Pi_k V_k^{v_k}. \quad (\text{E4})$$

Using (32), (33), and (E4), we have

$$\begin{aligned} \Pi[\text{diag}^{(i)}] &= 2I \left[S D^{I-1} \prod_k V_k^{v_k} \right] = 2I \frac{1}{D} \text{diag}^{(i)}, \\ \text{f}_j[\text{diag}^{(i)}] &= j! D^{-j} \left[v_j S D^I V_j^{v_j-1} \prod_{k \neq j} V_k^{v_k} \right] = j! v_j D^{-j} \frac{1}{V_j} \text{diag}^{(i)}. \end{aligned} \quad (\text{E5})$$

Substituting (E5) into the last line of (E3), we have

$$\text{EX}^{(i)} = \left(- \sum_{j=3}^n j v_j + 2I \right) \text{diag}^{(i)} \frac{1}{D} = 0, \quad (\text{E6})$$

where we have used (D1) with $E = 0$ in the last step.

The discussion above does not take into account the fact that Eq. (E5) can contain terms with different topologies and permutations [see (3) and the discussion which follows this equation]. For an arbitrary diagram in the effective action, the contribution to the self-energy that is produced by opening one line can be different, depending on which line is opened. We must show that each topology that is produced cancels individually. It is straightforward to see how this works. Consider the example where $\text{diag}^{(i)}$ is taken to be the graph EIGHT4 in Fig. 12. We consider the contribution to $\text{EX}^{(\text{EIGHT4})}$ from one line in the diagram and the two vertices this line attaches to, where the contribution to f_j from these vertices is divided by the numerical factor j . If we can show that these contributions cancel, then it is clear that the contributions from any and all lines and their vertex partners cancel. Note that the vertex contribution must be divided by the factor j because each vertex must partner with j different lines.

We consider the case where the designated line is the horizontal line in the EIGHT4 diagram. This diagram is redrawn in Fig. 30(a). The corresponding contribution to the self-energy is shown in part (b) of Fig. 30. The contributions to the functions f_5 and f_3 from the vertices which attach to each end of the designated line are shown in parts (c) and (d), where the index x indicates the leg of the vertex that was attached to the designated line in the original diagram in part (a). We substituting

the graph in part (c) into the right side of the Π -basketball diagram that contains two V_5 's and the graph in part (d) into the right side of the Π -basketball diagram that contains two V_3 's. These two substitutions produce the two different permutations that are indicated by the factor (2) in front of the diagram in part (b). The numerical factors are $(2) \cdot 1/8 - 1/4! \cdot 1/8 \cdot 5! \cdot [1/5] - 1/2! \cdot 1/8 \cdot 3! \cdot [1/3] = 0$.

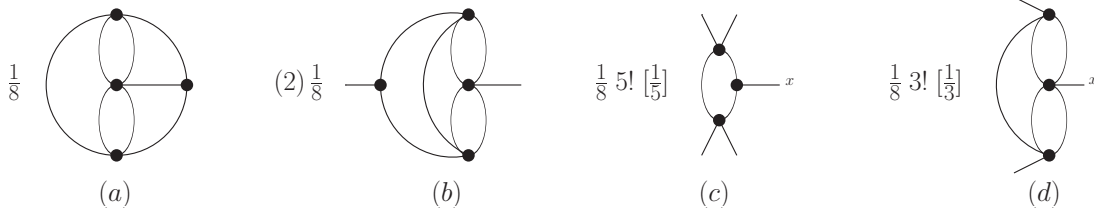


FIG. 30. The cancellation of one part of $\text{EX}^{(\text{EIGHT}^4)}$. The square brackets indicate the factors $1/j$ discussed in the text under Eq. (E6).

The procedure above can be applied to any line in any diagram. It is easy to see that the numerical factors are always correct to produce a cancellation. In the first line of Eq. (E5), a factor I is removed since only one line is differentiated. In the second line of Eq. (E5), a factor $j v_j$ is removed because only one vertex is differentiated, and the contribution is divided by $1/j$ (so it can be used $j - 1$ more times in partnership with the $j - 1$ other lines that connect to it). We obtain

$$\Pi[\text{diag}^{(i,l)}] = 2 \frac{1}{D} \text{diag}^{(i,l)}, \quad (\text{E7})$$

$$f_j[\text{diag}^{(i,l)}] = (j - 1)! D^{-j} \frac{1}{V_j} \text{diag}^{(i,l)},$$

where the notation $\text{diag}^{(i,l)}$ indicates that an arbitrary line labeled (l) in the diagram labeled (i) is considered. Using these results, (E6) becomes

$$\text{EX}^{(i,l)} = (-1 - 1 + 2) \text{diag}^{(i,l)} \frac{1}{D} = 0. \quad (\text{E8})$$

The two terms -1 in the equation above correspond to the two nonzero terms in the sum in (E6) which come from the two vertices that attach to the designated line.

Thus, we have proved that $\text{EX}^{(i)} = 0$ in (E3). Equivalently, we have shown that when we substitute (E2) into the vertex on the right side of each Π basketball in (E1), the sum of all terms produced by the functionals f_j cancel with the second sum in (E1).

We must also consider the term produced by the bare vertex from the first term on the right side of (E2). This term produces the two Π -basketball topologies which have a bare V_3^0 and V_4^0 on the right side. However, the second and third terms on the right side of (E1) contain two graphs each, which are Π -basketball topologies with the bare vertex on the left and right sides. The result is that the graphs with bare vertices on the right side cancel, and we are left with the graphs labeled (2) and (4) in Fig. 29.

Note that the HAIR diagram contains a bare vertex V_4^0 , and therefore the lines that attach to the bare vertex do not have partner contributions from a term of the form $f_4^{(\text{HAIR},l)}$, which means that $\text{EX}^{(\text{HAIR})} \neq 0$. As mentioned above, it is straightforward to show that $\text{EX}^{(\text{HAIR})}$ is diagram (3) in Fig. 29.

[1] C. DeDominicis and P.C. Martin, J. Math. Phys. (N.Y.) **5**, 14 (1964).

- [2] C. DeDominicis and P.C. Martin, J. Math. Phys. (N.Y.) **5**, 31 (1964).
- [3] R.E. Norton and J.M. Cornwall, Ann. Phys. (N.Y.) **91**, 106 (1975).
- [4] J. Berges and J. Cox, Phys. Lett. **B517**, 369 (2001) - *arXiv:hep-ph/0006160*.
- [5] G. Aarts and J. Berges, Phys. Rev. **D64**, 105010, (2001) - *arXiv:hep-ph/0103049*.
- [6] Alejandro Arrizabalaga, Jan Smit and Anders Tranberg, Phys. Rev. **D72**, 025014 (2005) - *Xiv:hep-ph/0503287*.
- [7] J. Berges, Sz. Borsanyi and C. Wetterich, Nucl. Phys. **B727**, 244 (2005) - *arXiv:hep-ph/0505182*.
- [8] Gert Aarts and Anders Tranberg, Phys. Rev. **D74**, 025004 (2006) - *arXiv:hep-th/0604156*.
- [9] Gert Aarts, Nathan Laurie and Anders Tranberg, Phys. Rev. **D78**, 125028 (2008) - *arXiv:0809.3390*.
- [10] M.E. Carrington and E. Kovalchuk, Phys. Rev. **D77**, 025015 (2008) - *arXiv:0709.0706*.
- [11] M.E. Carrington and E. Kovalchuk, Phys. Rev. **D80**, 085013 (2009) - *arXiv:0906.1140*.
- [12] M.E. Carrington and E. Kovalchuk, Phys. Rev. **D81**, 065017 (2010) - *arXiv:0912.3149*.
- [13] J. Berges, Sz. Borsanyi, U. Reinosa and J. Serreau, Phys. Rev. **D71**, 105004 (2005) - *arXiv:hep-ph/0409123*.
- [14] J. Berges, in *Introduction to Nonequilibrium Quantum Field Theory*, edited by M. Bracco, M. Chiapparini, E. Ferreira and T. Kodama, AIP Conf. Proc. **739**, 3 (AIP, New York, 2005) - *arXiv:hep-ph/0409233*.
- [15] J. Berges and J. Serreau, in *Proceedings of Strong Electroweak Matter*, edited by K.J. Eskola, (World Scientific, Singapore, 2004) - *arXiv:hep-ph/0410330*.
- [16] E. Calzetta, Int. J. Theor. Phys. **43**, 767 (2004) - *arXiv:hep-ph/0402196*.
- [17] U. Reinosa and J. Serreau, Ann. Phys. (N.Y.) **325**, 969 (2010) - *arXiv:0906.2881*
- [18] G. Aarts, D. Ahrensmeier, R. Baier, J. Berges and J. Serreau, Phys. Rev. **D66**, 045008 (2002) - *hep-ph/0201308*.
- [19] H. van Hees and J. Knoll Phys. Rev. **D66**, 025028 (2002) - *arXiv:hep-ph/0203008*.
- [20] M.E. Carrington and E. Kovalchuk, Phys. Rev. **D76**, 045019 (2007) - *arXiv:0705.0162*.
- [21] U. Reinosa and J. Serreau, JHEP, **0711**, 097 (2007) - *arXiv:0708.0971*.
- [22] J. Peralta-Ramos and E. Calzetta, J. Phys.: Condens. Matter **21**, 215601 (2009) - *arXiv:0811.2765v2*.
- [23] H. van Hees and J. Knoll, Phys. Rev. **D65**, 025010 (2001) - *arXiv:hep-ph/0107200*
- [24] H. van Hees and J. Knoll, Phys. Rev. **D65**, 105005 (2002) - *arXiv:hep-ph/0111193*.
- [25] J. Berges, S. Borsanyi, U. Reinosa and J. Serreau, Ann. Phys. (N.Y.) **320**, 344 (2005) - *arXiv:hep-ph/0503240*.
- [26] U. Reinosa and J. Serreau, JHEP **0607**, 028 (2006) - *arXiv:hep-th/0605023*.
- [27] A. Arrizabalaga and J. Smit, Phys. Rev. **D66**, 065014 (2002) - *arXiv:hep-ph/0301093*.
- [28] M.E. Carrington, G. Kunstatter and H. Zaraket, Eur. Phys. J. **C42**, 253 (2005) - *arXiv:hep-ph/0309084*.
- [29] J. Berges, Phys. Rev. **D70**, 105010 (2004) - *arXiv:hep-ph/0401172*.
- [30] M.E. Carrington, Eur. Phys. J. **C35**, 383 (2004) - *arXiv:hep-ph/0401123*.
- [31] M.E. Carrington and Yun Guo, Phys. Rev. **D83**, 016006 (2011) - *arXiv:1010.2978*.
- [32] D. Binosi and L. Theussl, Comput. Phys. Commun. **161**, 76 (2004) - *arXiv:hep-ph/0309015*.
- [33] P. Cvitanović, B. Lautrup and R.B. Pearson, Phys. Rev. **D18**, 1939 (1978).
- [34] K. Kajantie, M. Laine and Y. Schröder, Phys. Rev. **D65**, 045008 (2002) - *arXiv:hep-ph/0109100*.
- [35] R. Alkofer, M. Q. Huber and K. Schwenzer, Comput. Phys. Commun. **180**, 965 (2009).